HOLOCENE ENVIRONMENTAL VARIABILITY IN SUBALPINE ALBERTA: PROXY EVIDENCE FROM $\delta^{13}C$ AND $\delta^{18}O$ VALUES OF UPPER HOGARTH LAKE MARL

A Thesis Submitted to the College of
Graduate and Postdoctoral Studies
In Partial Fulfillment of the Requirements
For the Degree of Master of Science
In the Department of Geological Sciences
University of Saskatchewan
Saskatoon

By:

DUSTIN RON MATKOWSKI

PERMISSION TO USE

In presenting this thesis/dissertation in partial fulfillment of the requirements for a Postgraduate degree from the University of Saskatchewan, I agree that the Libraries of this University may make it freely available for inspection. I further agree that permission for copying of this thesis/dissertation in any manner, in whole or in part, for scholarly purposes may be granted by the professor or professors who supervised my thesis/dissertation work or, in their absence, by the Head of the Department or the Dean of the College in which my thesis work was conducted. It is understood that any copying or publication or use of this thesis/dissertation or parts thereof for financial gain shall not be allowed without my written permission. It is also understood that due recognition shall be given to me and to the University of Saskatchewan in any scholarly use which may be made of any material in my thesis/dissertation.

DISCLAIMER

This thesis was exclusively created to meet the thesis and/or exhibition requirements for the degree of Master of Science at the University of Saskatchewan. References in this thesis to any specific commercial products, process, or service by trade name, trademark, manufacturer, or otherwise, does not constitute or imply its endorsement, recommendation, or favoring by the University of Saskatchewan. The views and opinions of the author expressed herein do not state or reflect those of the University of Saskatchewan and shall not be used for advertising or product endorsement purposes.

Requests for permission to copy or to make other uses of materials in this thesis/dissertation in whole or part should be addressed to:

Head of Geological Sciences
University of Saskatchewan
Saskatoon, Saskatchewan S7N 5E2 Canada

OR

Dean
College of Graduate and Postdoctoral Studies
University of Saskatchewan
116 Thorvaldson Building, 110 Science Place
Saskatoon, Saskatchewan S7N 5C9 Canada

ABSTRACT

A 3.6-meter lake sediment core was recovered from Upper Hogarth Lake in the subalpine region of southwestern Alberta, Canada. The core provides proxy evidence for Holocene environmental variability over the last 12,000 years. The core was sub-sampled at millimeter resolution for $\delta^{18}O_{CaCO_3}$ and $\delta^{13}C_{CaCO_3}$ values, yielding over 750 samples for analysis. Variation in $\delta^{18}O_{CaCO_3}$ values record changes in the dominant seasonality of precipitation in the region as a result of changing temperatures and atmospheric circulation, while variability in $\delta^{13}C_{CaCO_3}$ values record changes in basin ecology, humidity, and soil moisture.

Upper Hogarth Lake (50.793˚N, -115.319˚W) is located approximately 100km WSW of the city of Calgary, Alberta in the Kananaskis Range of the Canadian Rocky Mountains. It is situated in Quaternary glacial till overlying Devonian-Carboniferous carbonate bedrock at an elevation of 1,900masl. Upper Hogarth Lake is dimictic, with a surface area of 0.026 km^2 and a maximum depth of <8m. It is hydrologically open with groundwater exchange and seasonal outflow. It is recharged via groundwater, snowmelt and rainfall. Precipitation of calcite that accumulates as marl occurs as encrustations on the macroscopic green algae *Chara sp*., with marl deposition beginning ~11,800 cal. yBP. The Upper Hogarth Lake age model was constructed using radiocarbon dating of eight terrestrial plant samples recovered from the core and by tephrochronology. Carbon-14 dates were calibrated to IntCal13 and plotted using the "Bacon" (v. 2.2) Bayesian Age-Depth Modelling package for "R" statistical software.

The core can be divided into 3 lithological zones: 1) basal diamict deposited following the retreat of the Cordilleran Ice Sheet; 2) inorganic mud, transitioning into organic gyttja deposited prior to 11,800 cal. yBP; and 3) cream-colored marl deposited from 11,800 cal. yBP to present. $\delta^{13}C_{CaCO3}$ values range from -4.1‰ to +3.2‰ VPDB, reflecting a basin ecosystem evolving toward modern conditions, as well as variability in local soil moisture and humidity. $\delta^{18}O_{CaCO_3}$ values range from -18.8‰ to -13.0‰ VPDB recording Early Holocene warming with summer precipitation dominating the lake water recharge. $\delta^{18}O_{CaCO_3}$ and $\delta^{13}C_{CaCO_3}$ values suggest warm, arid Mid-Holocene summers with snowmelt being the primary source of lake recharge. Late Holocene $\delta^{18}O_{CaCO_3}$ and $\delta^{13}C_{CaCO_3}$ values represent the onset of Neoglacial conditions with an increase in summer precipitation and humidity toward present.

ACKNOWLEDGMENTS

I would like to acknowledge the support, encouragement, and feedback of my supervisor, Dr. William Patterson. I am very grateful to him for this opportunity, for his tutelage, for his friendship and for including me in his other research ventures. I would also like to thank Dr. Sandra Timsic for all her help and guidance in data interpretation, conference preparation, writing, and lab work. Thank you to Dr. Chris Holmden and Dr. Jim Basinger for their time on my committee and for their helpful feedback.

Thank you to: Tim Prokopiuk for his advice and help with petrographic microscopy, Dr. Luis Buatois for his help with sedimentology and for lending me his microscope, Drs. Bernhard Mayer and Ann-Lise Norman at the University of Calgary for their perspective on Alberta precipitation, and Dr. Michael Bosilovich at NASA and Paul Dunphy at Calgary Global News for their advice regarding atmospheric circulation. Thank you to Doney Pan for her help with travel expenses associated with presenting my research at the AGU Fall Meeting.

This research was supported by funding provided by NSERC, the M.Sc. Graduate Scholarship and Graduate Teaching Fellowship Scholarship from the University of Saskatchewan - Department of Geological Sciences.

CONTENTS

TABLE OF FIGURES

LIST OF ABBREVIATIONS

BED-DIC	bedrock-sourced dissolved inorganic carbon
cal. yBP	calibrated years before physics (1950 C.E.)
cP	continental Polar
CPV	Circumpolar Vortex
DIC	dissolved organic carbon
GISP2	Greenland Ice Sheet Project Two
GRIP	Greenland Ice-core Project
HTM	Holocene Thermal Maximum (Hypsithermal)
IAEA	International Atomic Energy Agency
ka	kilo-annum (thousands of years ago)
LIA	Little Ice Age
MCA	Medieval Climate Anomaly
mP	maritime Pacific
mT	maritime Tropical
n.d.	“no date” (in a citation, typically a webpage)
NOAA	National Oceanic and Atmospheric Administration
NRC	NOAA Research Council
POC	particulate organic carbon
PPT	precipitation
RWP	Roman Warm Period
SEM	scanning electron microscope
SWE	snow-water equivalent
TPOC	terrestrial particulate organic carbon
UHL	Upper Hogarth Lake
VPDB	Vienna Pee Dee Belemnite
VSMOW	Vienna Standard Mean Ocean Water
WC	weathered carbon

CHAPTER 1 INTRODUCTION

As the World's population continues to increase rapidly, the stress on Earth's fresh water resources is exacerbated. Understanding how freshwater ecosystems have responded to natural climate variations of the past is essential for predicting their response to future stresses caused by anthropogenically induced climate change and the increased demand for fresh water. To best understand climate variability, requires development of high-resolution climate proxy data sets from populated, mid-latitude regions of the world where global climate change may have a profound societal, environmental, and economical effects (Kirby et al., 2002).

1.1 Objectives and Motivation

The timing and nature of vegetation responses to Late Glacial and Holocene climate change in the central Rocky Mountains are not resolved in detail. High-resolution paleoenvironmental reconstructions for the region are required for evaluation and validation of earth system models (Reasoner and Huber, 1999). This study endeavors to increase our understanding of the seasonal variability of mid-latitude, continental precipitation and how carbon isotope values of lacustrine calcite may be used as proxy evidence for variability in regional humidity and soil moisture. Reliable and steady moisture supply to continental interiors from the Earth's oceans is essential for terrestrial ecosystems and human society. The key issue in forecasting future water supplies from alpine areas in western North America is predicting future winter precipitation scenarios under forecasted Global Warming scenarios (Lapp et al., 2002). Identification of continental precipitation sources has received increased attention in recent years. Utilizing various numerical methods, precipitation sources have been characterized at regional to global scales (Van Der Ent and Savenije, 2013). As part of a 2010 study, the Bow River Basin Council found that the issues of greatest concern for the watershed are: protection of the headwaters, the impacts of climate change on glaciers, and managing the impact of increasing population on freshwater resources (Bow River Basin Council, 2010). Most large continental areas obtain moisture from just one or two sources with seasonal variation. Changes in atmospheric circulation induced by Global Warming will redirect atmospheric water vapor trajectories. Continental regions that receive moisture from only one or two source regions may be more significantly affected by changes in water cycle due to changing climate than regions that draw moisture from multiple sources (Gimeno et al., 2012).

Nearly 8% of Canada's surface area is occupied by lakes and wetlands, comprising a significant portion of the catchment land surface and representing a significant proportion of the World's fresh water. Lakes cause modifications to the quantity and quality of water as it flows through a catchment (Kendall and McDonnell, 1998). It is therefore imperative to understand how they respond to environmental change, if we are to better predict future water supplies. Lakes have always been subject to the influence of climate change, with natural climate variability in the past representing a primary reason that lakes are ephemeral features of the landscape (Vincent, 2009). Future changes in the amount, seasonality and quality of water supplies will be critical determinants of human activities. Increasing demand coupled with changes in both the volume and timing of runoff will create severe water supply problems that will require effective management and mitigation strategies (Barnett et al., 2004; Watson and Luckman, 2006).

The main challenge to identifying causes of Holocene climate variability has been the lack of high-resolution records that extend beyond meteorological and tree-ring chronologies (Asmerom et al., 2007). This study will show that the Holocene was not unremarkable with respect to climate variability. Studies of the GISP2 and GRIP ice cores often neglect to report any substantial variability in the Holocene record (Grootes et al., 1993). Climate determines many of the characteristics of lakes, their biota, catchment dynamics forced by temperature shifts, alteration of the chemical composition, and nutrient status of the water through increased evaporation rates during warm arid periods, or by dilution during wet intervals (Hickman and Reasoner, 1998). 20^{th} century warming is likely to have been the largest of any century during the last 1000 years (Houghton et al., 2001).

CHAPTER 2 THEORY AND METHODS

2.1 Theory

Lacustrine carbonates offer one of the most abundant geochemical archives of terrestrial paleoenvironmental data (Hren and Sheldon, 2012). Trace elemental and stable isotope chemistry of calcium carbonate archives information about past hydrology, meteorology, seasonality, temperature, ecosystem succession, and the carbon cycle ((Diefendorf et al., 2007; Epstein et al., 1953; Kirby et al., 2002; Leng and Marshall, 2004; McCrea, 1950; Stuiver, 1970; Talbot, 1990). Freshwater lakes may preserve high-resolution records dating back to their formation if accumulation of carbonate is continuous and undisturbed. To date, ocean sediment has been more commonly studied as a paleoclimate proxy because variability in $\delta^{18}O_{H2O}$ values of freshwater lakes associated with climatic changes is much greater than variability in oceanic $\delta^{18}O_{H2O}$ values (Stuiver, 1970). Selection of an appropriate lake, and coring methodology, is critical for a successful study. Choosing a lake with a limited number of variables simplifies the interpretation of isotopic data from the carbonate. For a researcher to ascribe isotopic variation in the core to a particular forcing mechanism requires that all factors that may force the variation be considered. Ideally a lake with a known (or predictable) hydrologic history would provide for a simpler reconstruction of environmental history. Unchanging geomorphology is also ideal, as a lake or surrounding area that is frequently disturbed tectonically can influence variables such as sediment influx, sedimentation rate and the potential for the preservation of any primary sedimentary structures. Lakes with limited bioturbation are preferred because re-working of the sediment, likewise, erases primary sedimentary structures, decreasing the resolution of the data, and obfuscating the primary paleoenvironmental record. An understanding of the mechanism of calcium carbonate production in the lake is important for an appropriate interpretation of the isotope record.

In this study, a subalpine marl lake was selected for coring as they are sensitive recorders of past environmental variability (Hickman and Reasoner, 1998). Marl lakes are hard-water, often dimictic systems with calcium carbonate mud deposited as prograding benches underlying shallow water, within the photic zone. The are commonly found within kettle holes in glacial drift in regions of carbonate bedrock where accumulation of nearly pure (~90%) low-magnesium calcite may persist through the Holocene (Drummond et al., 1995; Murphy and Wilkinson,

1980). Most marl lakes are groundwater seepage lakes that lack significant fluvial inflow-outflow systems where groundwater percolation through surrounding carbonate rich gravels and soils enriches the groundwater in calcium and bicarbonate ions. During spring turnover, cold epilimnic waters warm and degas CO_2. Degassing of aqueous CO_2 causes the water to become supersaturated with respect to calcite (Drummond et al., 1995; Murphy and Wilkinson, 1980). More importantly for our purposes, the bulk of the carbonate produced in Hogarth Lake forms as an extracellular precipitate on the stems of macrophyte green algae.

The lake selected for this research project is ideal in terms of its topographic isolation, its simple hydrology and its internal dynamics. The lake is a groundwater-fed kettle lake situated in Carboniferous bedrock in a valley of the Canadian Rocky Mountains. Subalpine lakes are sensitive recorders of past environmental changes (Hickman and Reasoner, 1998). Abundant calcium (Ca^{2+}) and bicarbonate (HCO_3^-) ions are delivered in solution to the lake via groundwater infiltration through the surrounding carbonate rich soils and gravels. The mechanism of carbonate precipitation is also ideal for archiving paleoenvironmental variability. Seasonal precipitation of authigenic calcite occurs as bio-induced encrustations on the charophyte *Chara corallina*. This is the predominant source of calcium carbonate, with minor contributions from shells of gastropods, ostracods and molluscs. Evidence of the existence of these charophytes is observed in the UHL core as deep as 2.6m, corresponding to an extrapolated age of 11,800 cal. yBP. Charophytes are sensitive to ecological change and are useful paleolimnological markers (García, 1994). This species is important because of the way they perform photosynthesis in the littoral zone of the lake. Carbonate calcification accompanies the photosynthetic utilization of bicarbonate on a 1:1 ratio with photosynthesis (Mcconnaughey, 1991; Mcconnaughey et al., 1991; McConnaughey et al., 1994; Pełechaty et al., 2013). As Chara occur only in the littoral zone of the lake, the carbonate encrustations will reflect the isotopic value of the water above the hypolimnion. As calcite is precipitated extracellularly, the calcite encrustations on *Chara sp.* are known to precipitate in isotopic equilibrium with the surrounding waters (Drummond et al., 1995; Leng and Marshall, 2004; Mullins et al., 2011). Marl accumulation occurs via disarticulation and deposition of the calcified charophytes (Davis, 1900; Murphy and Wilkinson, 1980), with the encrustations accounting for up to 75% of charophyte dry weight (Pełechaty et al., 2013).

2.2 Stable Isotopes

The use of $\delta^{18}O_{CaCO_3}$ values for paleoenvironmental reconstruction has a long history dating back to ideas proposed by Urey (1947). In 1964, Dansgaard published "Stable isotopes in precipitation", establishing the foundation for future research on stable isotopes in natural waters along with Craig (1961), Gonfiantini (1978) and Rozanski et al. (1993). Subsequent to Urey's landmark paper, advances were made with respect to understanding the fractionation between water and carbonates (Epstein et al., 1953; McCrea, 1950; Stuiver, 1970; Talbot, 1990). The IAEA defines isotopic fractionation as "the phenomenon that the isotopic composition of an element in a certain compound changes by the transition of the compound from one physical state or chemical composition to another" (International Atomic Energy Agency, 2013). The two main mass-dependant isotope fractionation effects are kinetic and equilibrium (thermodynamic) isotope effects. Isotopic equilibrium conditions exist where there is no net chemical reaction, but an exchange of isotopes between phases still occurs. Kinetic isotope effects are typically associated with fast, incomplete and/or unidirectional processes such as evaporation, diffusion and dissociation reactions. Kinetic fractionation effects consist of variations in strengths of bonds and reaction rates. The surface of any body of water will be subject to kinetic isotope effects during evaporation, in that $^{1}H^{1}H^{16}O$ molecules transfer into the vapor phase more commonly than the $^{1}H^{2}H^{16}O$ or $^{1}H^{1}H^{18}O$, resulting in an increase in the $\delta^{18}O_{H_2O}$ value of the remaining liquid water (Dansgaard, 1964). Biological isotopic fractionations, "vital effects", are another example of a kinetic isotope effect. Many carbonate producing organisms (e.g. mollusks) impart vital effects upon the precipitated carbonate as a result of their biological processes, and the isolation of the carbonate precipitation from the external environment. Such biological influence is not expected to have a significant effect on the sediment analysed in this study, because the carbonate is precipitated extracellularly in the water column.

In this paleoclimate study, I am principally concerned with $\delta^{18}O_{CaCO_3}$ and $\delta^{13}C_{CaCO_3}$ values derived by analysis of lacustrine carbonate sediment. $\delta^{18}O_{H_2O}$ values are determined relative to international standards such as Vienna Standard Mean Ocean Water (VSMOW), Vienna Standard Light Antarctic Precipitation (VSLAP) for $\delta^{18}O_{H_2O}$, and Vienna Peedee Belemnite (VPDB) for $\delta^{18}O_{CaCO_3}$ and $\delta^{13}C_{CaCO_3}$ values. Carbonate aliquots are converted to CO_2 by reaction with 105% anhydrous phosphoric acid, then injected into the mass spectrometer

where the sample CO_2 is compared to a laboratory standard CO_2 that has been calibrated to the international standards and written in "delta" (δ) notation (Eqn. 1).

$$\delta^{18}O_{sample-standard} = \left[\frac{\left(\frac{^{18}O}{^{16}O}\right)sample}{\left(\frac{^{18}O}{^{16}O}\right)standard} - 1\right] * 1000‰ \qquad \text{(Equation 1)}$$

2.3 $\delta^{18}O_{CaCO_3}$ and $\delta^{13}C_{CaCO_3}$ values of Upper Hogarth Lake Marl

A number of important characteristics of the mid-latitude, subalpine hydrologic system in this study include: 1) fresh waters generally exhibit lower $\delta^{18}O$ values than sea water; 2) $\delta^{18}O_{H_2O}$ values of precipitation decrease with decreasing temperature of condensation; 3) $\delta^{18}O_{H_2O}$ values decrease with increasing altitude and latitude; and, 4) there is considerable seasonal variation in $\delta^{18}O_{H_2O}$ values of precipitation at high altitudes (Dansgaard, 1964). Although, altitude and latitude influence $\delta^{18}O_{H_2O}$ values of precipitation, neither have changed over the last 12,000 years. The dominant forcing mechanisms driving $\delta^{18}O_{lake\ water}$ values are the dominant seasonality of precipitation and changes in moisture source, because of shifting atmospheric circulation, conflated with the influence of changes in atmospheric temperatures. Seasonal variability in $\delta^{18}O_{H_2O}$ values of precipitation forces a portion of the variability in lake waters, recorded by carbonate sediment (Stuiver, 1970). $\delta^{18}O_{CaCO_3}$ values in this study will be used to infer changes in atmospheric circulation, meteoric patterns and water (atmospheric) temperature. Kinetic fractionation related to evaporation is most significant in hot and/or arid environments as will be discussed in greater detail in the results section. $\delta^{13}C_{CaCO_3}$ values are used to characterize the local carbon cycle, relative humidity and soil moisture. Information about changes in relative humidity and soil moisture are inferred based on the $\delta^{13}C$ values of local plant material contributed to soil that breaks down into CO_2, particulate organic matter (POC), and dissolved organic matter (DOC) that enter the lake carbon budget. $\delta^{13}C$ values of plant tissue reflect the photosynthetic pathway that are in turn be determined by temperature, soil moisture, and relative humidity.

2.4 Calcite Precipitation

UHL calcite is precipitated extracellularly on *Chara sp.* as a by-product of photosynthesis, thus it represents a "biologically-induced" calcite. $\delta^{18}O_{CaCO_3}$ values of biologically-induced calcite in lacustrine sequences have become a valuable tool for reconstructing high-resolution paleoenvironmental variability in continental areas, due to the rapid response of lake ecosystems to environmental perturbations (Teranes et al., 1999). As calcite is precipitated in equilibrium with the water column, $\delta^{18}O_{CaCO_3}$ will depend primarily on $\delta^{18}O_{\text{lake water}}$ values with some temperature overprinting (e.g. Leng and Marshall, 2004). With respect to temperature, carbonates have a long history of use as paleothermometers (Epstein et al., 1953; Kim and O'Neil, 1997; Leng and Marshall, 2004; McCrea, 1950; Stuiver, 1970; Urey, 1947). Kim & O'Neil (1997) refined the earlier equations of Urey, Epstein, Lowenstam and others (Eqn. 2). If the $\delta^{18}O_{H_2O}$ value of the water and associated calcite are known, the temperature at the time of precipitation can be calculated using the appropriate fractionation factor: $\alpha_{\text{calcite-water}}$. That fractionation factor α is described by Kim & O'Neil as:

$$1000ln\alpha_{calcite-water} = 18.03(10^3T^{-1}) - 32.42 \qquad \text{(Equation 2)}$$

where T is the temperature in Kelvin (for temperatures < 25°C) (Kim and O'Neil, 1997).
The fractionation factor, α, represents the partitioning of isotopes of an element undergoing a phase change at equilibrium. The fractionation factor for calcite-water, where calcite is the product and water the reactant, is obtained from:

$$\alpha_{calcite-water} = \frac{1000+\delta^{18}O_{calcite}}{1000+\delta^{18}O_{water}} \qquad \text{(Equation 3)}$$

A significant challenge exists in constraining $\delta^{18}O_{\text{lake water}}$ before temperature can be calculated. This is accomplished in several ways, such as paired-species analyses (Smith and Patterson, 1994), use of an accretionary carbonate that has a specific shutdown temperature (Patterson et al. 1993; Dettman et al., 1999), clumped isotopologue chemistry (e.g. Eiler, 2007; Csank et al., 2011), thermal preference/tolerance of organisms (Patterson et al., 1993), and decrepitation of fluid inclusions (e.g. Affolter et al., 2014). Theoretical $\delta^{18}O_{\text{lake water}}$ values calculated using UHL

$\delta^{18}O_{CaCO_3}$ values requires a variation in temperature far too large to be the dominant forcing mechanism. Thus, this record of $\delta^{18}O_{CaCO_3}$ values is one dominated by variability in water (source and seasonality) with a thermal overprinting.

2.5 Methods

A 3.6m long lake sediment core was recovered via Vibracoring (Smith, 1998), in a 10.2cm aluminum pipe and transported to the University of Saskatchewan where it was longitudinally split, photographed, logged, and visually described. The age model was developed using ^{14}C data from 8 samples of terrestrial plant matter recovered from the core (Fig. 2.1). Samples were radiocarbon dated by the Institute of Physics Radiocarbon Laboratory in Gliwice, Poland. ^{14}C values were calibrated and plotted using the "Bacon" (v. 2.2) Bayesian Age-Depth Modelling package for "R" statistical software. ^{14}C ages were calibrated using the IntCal13 Northern Hemisphere atmospheric radiocarbon calibration curve (Reimer et al., 2013). The age model infers an age of 7,600 cal. yBP for the Mazama tephra, in agreement with other studies (Egan et al., 2015; Zdanowicz et al., 1999). The Mazama tephra was identified using an SEM and a petrographic microscope, observed as thin bubble-wall glass shards (e.g. Reasoner and Healy, 1986; Zdanowicz et al., 1999). The oldest calibrated date obtained was 10,545 cal. yBP. A linear regression ($R^2 = 0.9999$) was used to extrapolate dates (for similar lithology) earlier and later than the first and last ^{14}C dates for a total record that dates back to 11,800 cal. yBP.

Due to a lack of terrigenous material suitable for ^{14}C dating below a depth of 2.36m, dates older than 10,500 cal. yBP are extrapolated using the sedimentation rate determined from the carbon dates above, a reasonable assumption given little variation in sedimentation rate throughout the marl unit. Precise timing of deglaciation, and thus the origin of the lake, is difficult to estimate at the geographic location of Upper Hogarth Lake. The chronology of retreat of the east and south margins of the Cordilleran Ice Sheet remains poorly constrained due to the paucity of radiocarbon ages in that region and the complex interplay between alpine Rocky Mountain glaciers and lobes of the interior Cordilleran ice (Clague, 2017). The age model was used in combination with linear regression analysis ($R^2 = 0.9973 – 1$) using Prism 7 for Windows GraphPad software to estimate rates of deposition (Fig. 2.2). One ^{14}C value (in red, Fig. 2.1) is incongruent with other values by almost 1000 years for unknown reasons, but it was included for the sake of transparency.

Over 750 samples were retrieved at 1mm to 5mm intervals to generate the record of $\delta^{18}O_{CaCO_3}$ and $\delta^{13}C_{CaCO_3}$ values at the Saskatchewan Isotope Laboratory. Approximately 20-50µg of sediment was loaded into stainless steel cylinders and heated at 200°C in vacuo to remove organics and volatiles that may interfere with interpretation of the carbonate data. The samples were then placed into borosilicate glass vials to be auto-sampled by a Thermo Scientific™ Kiel IV carbonate device directly coupled to a Thermo Scientific™ MAT-253 dual-inlet stable isotope ratio mass spectrometer (SIRMS). Carbonate samples were reacted with 105% anhydrous phosphoric acid at 70°C for 420 seconds generating CO_2 that is cryogenically scrubbed to remove water and other volatiles that may influence $\delta^{18}O_{CaCO_3}$ and $\delta^{13}C_{CaCO_3}$ values. Values are reported in per mille (‰) notation relative to the Vienna Peedee Belemnite (VPDB), the international standard NBS-19, and internal standards. Isotope ratios are corrected for acid fractionation and ^{17}O contribution using the Craig correction (Craig, 1957). Precision is ~0.04‰ for $^{13}C/^{12}C$ and ~0.08‰ for $^{18}O/^{16}O$ (n=46, 1σ).

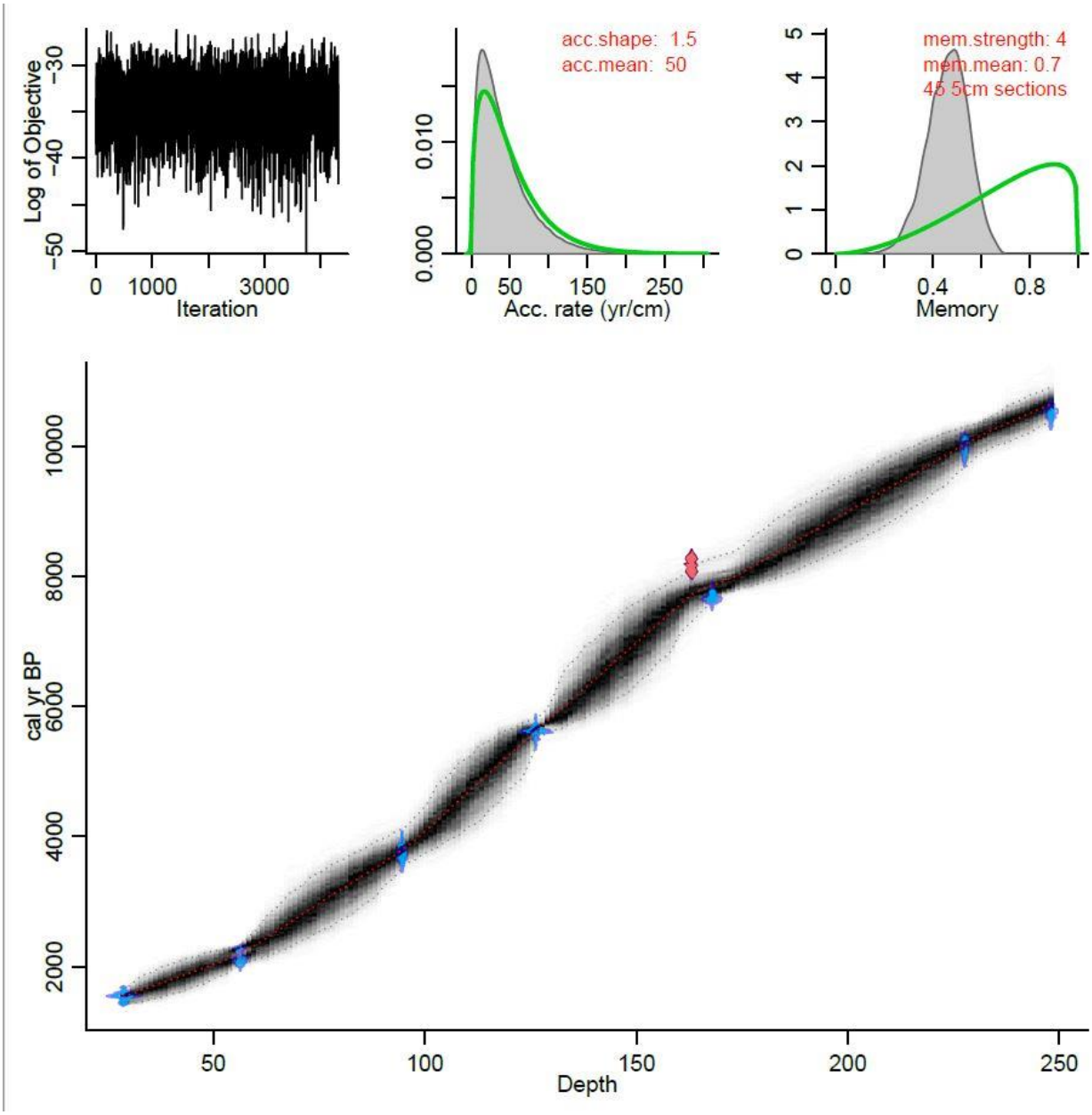

Figure 2.1. Age - Depth Model. Age in calibrated years before physics (1950 C.E.). 14-Carbon ages of 8 terrestrial plant matter samples (blue and red diamonds) were determined by the Institute of Physics Radiocarbon Laboratory in Gliwice, Poland. 14-Carbon ages were calibrated to the IntCal13 Northern Hemisphere atmospheric radiocarbon calibration curve (Reimer et al., 2013). Depth of lake sediment below water interface in centimeters. Image generated using Bacon" (v. 2.2) Bayesian Age-Depth Modelling package for "R" statistical software.

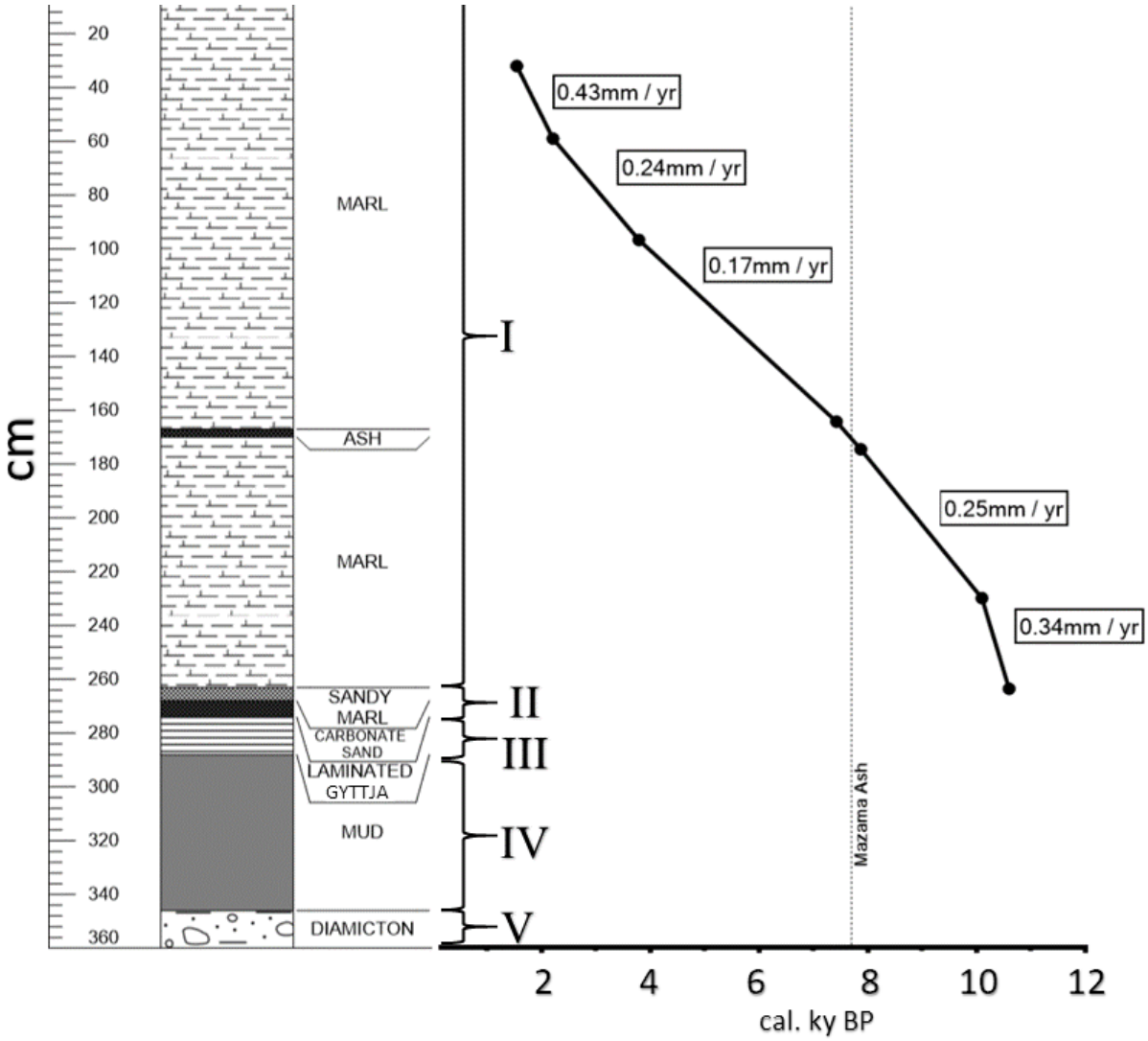

Figure 2.2. Core log and rates of deposition. Depth in centimeters below sediment-water interface. I: marl, II: sandy-marl transition, III: laminated gyttja, IV: non-laminated mud, V: basal glacial diamicton.

CHAPTER 3 STUDY AREA AND CORE DESCRIPTION

3.1 Study Area

3.1.1 Geography and Geology

Upper Hogarth Lake (UHL) (50.793˚N, -115.319˚W) is a groundwater fed, freshwater kettle lake in southwestern Alberta, Canada – approximately 100km WSW of Calgary (Fig. 3.1). It is the southernmost of the three Hogarth Lakes, situated in a valley at approximately 1900mASL in the Kananaskis Range of the Canadian Rocky Mountains.

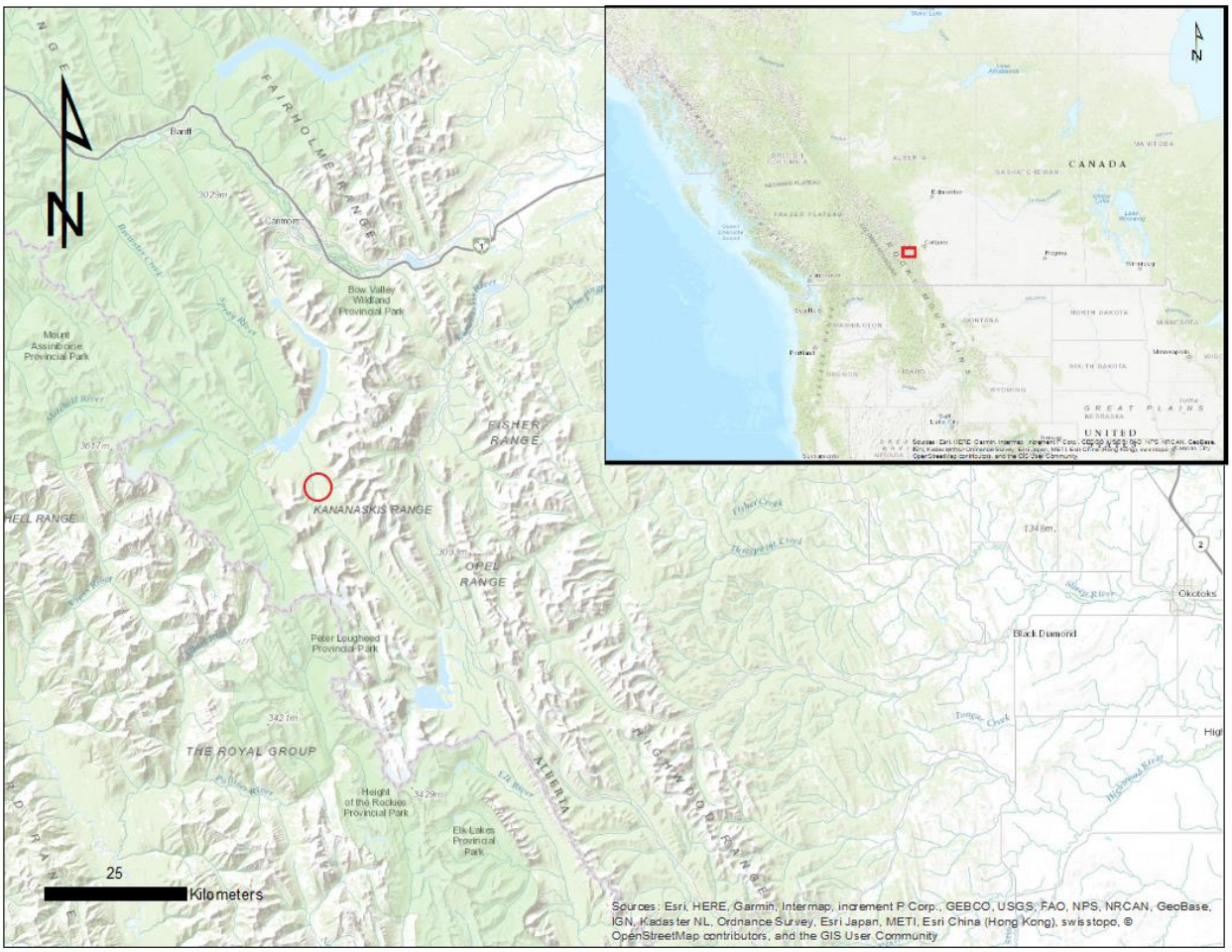

Figure 3.1. Study area (red circle) in the Kananaskis Range of the Alberta Rocky Mountains.

It is a protected area within Peter Lougheed Provincial Park. The region is characterized by Carboniferous bedrock covered in Quaternary glacial sediment.

3.1.2 Hydrology

UHL has a surface area of approximately 0.026km^2 and a maximum depth of < 8 m. It is hydrologically open, recharged via groundwater infiltration (snowmelt and rainfall) and precipitation, with spring/summer outflow. The Hogarth Lakes are situated in glacial till, classified as an alluvial fan aquifer (Toop and de la Cruz, 2002).

Bicarbonate and calcium ions from local carbonate rich soil and gravel are subsequently transported in solution to the lake. In this subalpine environment, rapid flow-through shallow groundwater paths are dominant, with variability in the contribution of groundwater dependent upon seasonality, rainfall and snowmelt amounts (Hood et al., 2006). Outflow occurs by seepage and spring/summer overflow north to Middle Hogarth Lake and the Lower Hogarth Lake marshland. The Hogarth Lakes are situated in the headwater region of the Bow River Basin watershed. Therefore, its location is ideal for evaluating the water isotope record before evaporative effects increase the $\delta^{18}O_{H_2O}$ values. Based on area, depth and recharge mechanisms (e.g. Lischeid et al., 2018), UHL residence time is estimated to be about one year, allowing for a rapid response to climate variables recorded as high-resolution variability in $\delta^{18}O_{CaCO_3}$ and $\delta^{13}C_{CaCO_3}$ values. Topographic characteristics of the area around the lake induces high rates of groundwater outflow and short residence times (e.g. Shapley et al., 2009). The lake is dimictic with wind and thermal driven mixing of surface and bottom water occurring twice per year.

3.1.3 Modern Meteorology and Climate

The Hogarth Lakes region is considered subalpine, with cool summers and snowy spring and autumn seasons with abundant winter snowfall (Downing and Pettapiece, 2006; Reasoner and Huber, 1999). The lake is often ice covered until mid-June, icing over again in November. From 1981 to 2017 average daily temperatures for the region ranged from -11°C in December to 13°C in July, with typical minimum and maximum values of -15°C and 19°C respectively (Alberta Agriculture and Forestry and Environment and Parks, n.d.).

Annual precipitation is currently dominated (between 50 and 80%) by snow (Bow River Basin Council, 2010; Toop and de la Cruz, 2002), with the snow water equivalent (SWE) of the cumulative snowpack reaching peak amounts in May (Pomeroy et al., 2016). The alpine and subalpine regions receive more winter precipitation than any other region of Alberta with common amounts of 650-750 mm (SWE) (Toop and de la Cruz, 2002). Snowfall and freezing temperatures are possible year-round but are least likely in July (Toop and de la Cruz, 2002). Summer precipitation is heaviest in July (400-550 mm) (Toop and de la Cruz, 2002). Present day low altitude winds are from the south with an annual average wind speed of 7km/h at 10m above ground (Alberta Agriculture and Forestry and Environment and Parks, n.d.). At present, cold winters and cool summers limit evaporation (Toop and de la Cruz, 2002).

The region is influenced by one, or a combination of 3 dominant air masses (Fig. 3.2): 1) Continental Polar (cP); 2) Pacific Maritime (mP); and, 3) Maritime Tropical (mT), (Peng et al. 2010). Seasonal variability and position of the North Polar Jet Stream determine the dominant air mass, both seasonally and secularly. During winter, the cold and dry Continental Polar air mass dominates most of Alberta, interrupted occasionally by “Chinook” winds. A Chinook wind is a parcel of warm and dry, often fast moving, air that descends the lee side of the Rocky Mountains through lower elevation areas, originating as moist air over the Pacific Ocean but drying due to orographic rain-out events. As the air descends it warms adiabatically, further decreasing relative humidity. Precipitation in the Hogarth Lakes region is sourced from a combination of the Pacific Ocean, the Gulf of Mexico and convective summer precipitation sourced from evapotranspiration over the Great Plains (Moran et al., 2007; Peng et al., 2004).

An oceanic area is considered a significant source of continental moisture when, on average, more than 20% of the total evaporation, and at least 250mm/yr of evaporation ends up as continental precipitation (Van Der Ent and Savenije, 2013). Moist air may be delivered to the

west coast of North America from the tropical Pacific by “atmospheric rivers” (Kamae et al., 2017). A Pacific atmospheric river (water vapor) known as the “Pineapple Express”, can drive warm moist equatorial Pacific air inland, likely traveling northeast through the Columbia River Gorge (National Oceanic and Atmospheric Administration (NOAA) and (NRC), 1985), and northward via the Rocky Mountain Trench between the Cascades and Rocky Mountain ranges into southern Alberta. It is transported via the westerly winds and the propagating wave movement of the jet stream. Moist summer air sourced from evapotranspiration (moisture recycling) over the American Great Plains and the heavily forested Rocky Mountains of the USA can be delivered into southern Alberta via an easterly upslope flow caused by cyclonic atmospheric circulation over the western United States (Milrad et al., 2015; Moran et al., 2007; Thériault et al., 2018). Moist air may also travel northward from the Gulf of Mexico across the Great Plains (Scott, 2013). During periods of enhanced meridional atmospheric flow, high pressure air masses can push far into northern Canada bringing increased temperatures to areas as far north as Yukon and Northwest Territories. When warm and moist air from the Gulf of Mexico is transported north, precipitation occurs as the air is forced upward over the Rocky Mountains, cooling adiabatically to saturation. This process can be enhanced when a counter-clockwise rotating low-pressure system centered over the Pacific Northwest United States pulls the moist Gulf air into Alberta (Scott, 2013; Thériault et al., 2018). Such an event occurred in June of 2013, where an air mass carrying moisture from the Gulf of Mexico delivered increased precipitation to the region causing catastrophic flooding along the Bow River and in Calgary. Temperature and precipitation variability in the Canadian Rocky Mountains are forced by changes in the position of the Circumpolar Vortex and atmospheric circulation, e.g., zonal atmospheric winds bringing winter precipitation but blocking summer easterly and southerly upslope moisture.

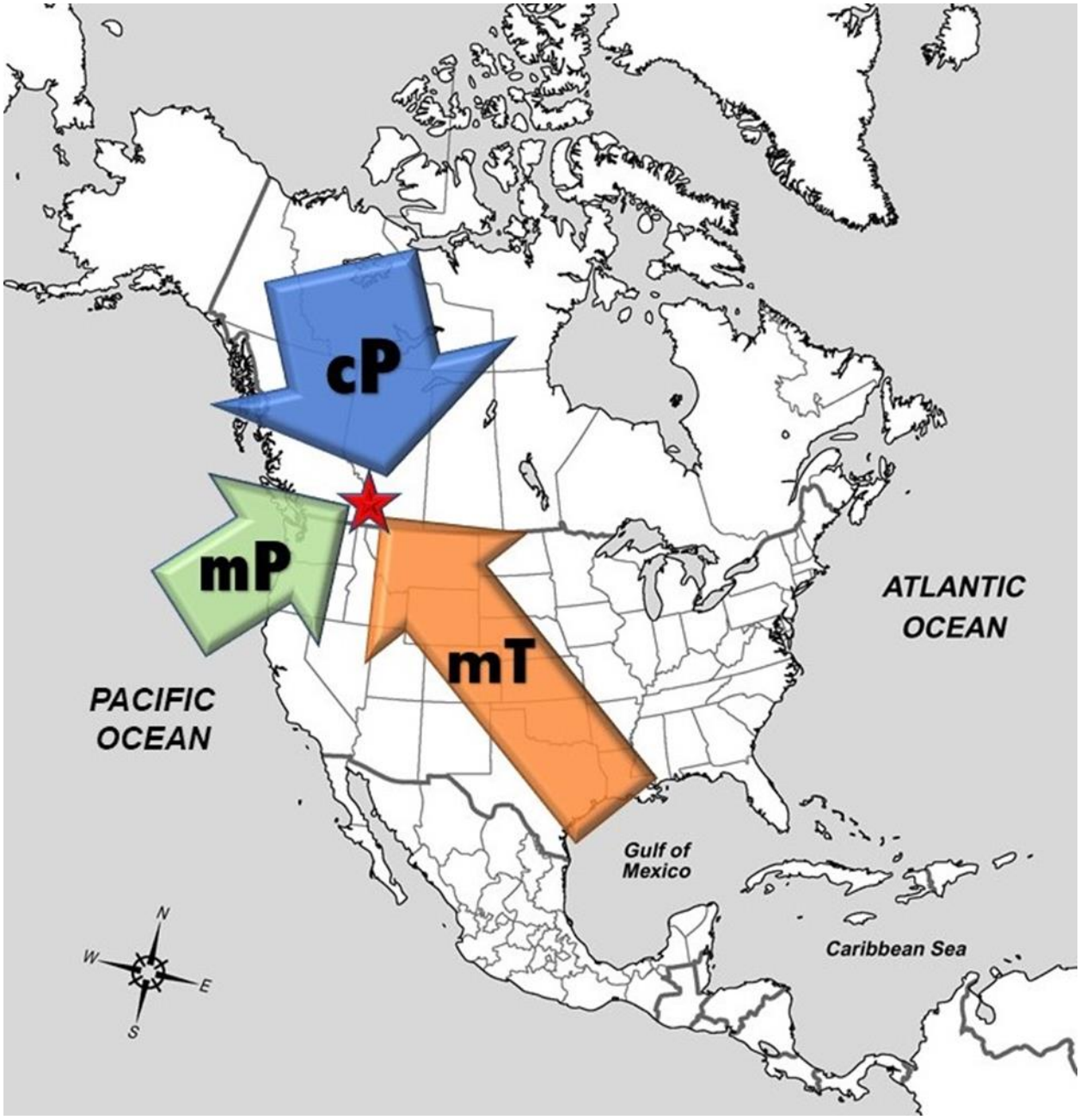

Figure 3.2. Dominant air masses over UHL (red star). Continental Polar (cP), Maritime Pacific (mP), Maritime Tropical (mT), after Peng et al., 2004.

3.1.4 Vegetation

The Hogarth Lakes lie in the Cordilleran Ecoclimatic Province (Downing and Pettapiece, 2006), presently characterized by cool summers with a growing season between late June and September. The area is dominated today by coniferous forest; blue spruce (*Picea engelmannii*), subalpine fir (*Abies lasiocarpa*), subalpine larch interspersed with herb-rich meadows, and fire-successional lodgepole pine (*Pinus contorta*) stands (Beaudoin and King, 1994; Downing and Pettapiece, 2006). Vegetation on the lower slopes is dominated by shrub willows (*Salix sp.*) and other shrubs including dwarf birch (*Betula glandulosa*) (Beaudoin and King, 1994). Wetland areas such as the area north of Upper Hogarth Lake are populated by sedges (*Cyperaceae*) (Beaudoin and King, 1994). The geographic location of UHL is such that vegetative species will be comprised predominantly of woody plants utilizing the C_3 photosynthetic pathway.

3.2 Core Description and Depositional History

The 3.6m Upper Hogarth Lake core can be subdivided into 5 general lithological zones (Fig. 2.2). Beginning at the base of the core with zone V are gravel and sands interpreted to represent the basal diamict, composed of glacially eroded carbonate bedrock. This is supported by similar $\delta^{18}O_{CaCO_3}$ (≈ -8.5‰VPDB) and $\delta^{13}C_{CaCO_3}$ values (≈ 0.5‰VPDB) to local sands and gravels at the study site (n = 9). Above that, in zone IV (3.47-2.88m) lies grey and beige inorganic mud with no discernable sedimentary structures or textures. This mud represents inorganic sediment deposited in the basin, in association with the expansion of alpine glaciers and the Crowfoot Advance (Younger Dryas Chron) (Reasoner and Huber, 1999). The beginning of zone III is marked by a distinct thin (2mm) black laminae at 2.88m. Zone III consists of dark grey-green and brown beds of gyttja, interpreted as an evolving lake bottom, and increasing biologic activity in the surrounding terrestrial ecosystem (e.g. Borzenkova et al., 2015). Zones III, IV, and V are characteristic of other similar lakes in the region (Beierle et al., 2003; Leonard and Reasoner, 1999; Reasoner and Huber, 1999). Zone II is interpreted as a transitional section where marl deposition began, indicated by the first signs of calcified charophyte stems (e.g., Borzenkova et al. 2015; Diefendorf et al. 2007; Hammarlund et al. 1997), and fine-grained calcite, are observed amongst a brown resinous sediment at 2.67m. This brown sediment is coincident with a 6‰ increase in $\delta^{13}C_{CaCO_3}$ values, indicative of an evolving carbon cycle. As the

lake water became clearer, charophyte algae colonized the littoral zone of the lake. In a similar lake, it was found that an increase in light availability occurs simultaneously with the development of dense beds of *Chara* vegetation (Blindow et al., 2002). In clear, oligotrophic lakes, charophytes may colonize lake bottoms to depth of 30m or more (Wehr and Sheath, 2015). The core transitions to Zone I (marl) at 2.67m, persisting to the top of the core, interrupted only by the Mazama ash (~7,600 cal. yBP; Egan et al., 2015; Zdanowicz et al., 1999) at 1.68m. Zone I consists of cream-colored, homogeneous marl sourced from calcite encrustations on charophyte algae.

CHAPTER 4 CARBON ISOTOPE RECORD OF UPPER HOGARTH LAKE MARL

4.1 $\delta^{13}C$ Values of Marl

$\delta^{13}C$ profiles of lake sediment have become a critical tool for paleoenvironmental reconstructions because lake carbon budgets are sensitive to climate (Diefendorf et al., 2007). $\delta^{13}C_{CaCO_3}$ values of UHL marl are interpreted to represent variation in soil moisture, regional humidity, carbon budget, and landscape evolution of the lake catchment area throughout the Holocene. UHL is an open carbonate system, described as "Case 2" and "Case 3" by Garrels and Christ (1965). Case 2 describes natural lake water in contact with the atmosphere, where the pH of the system is controlled by carbonate equilibria. Case 3 incorporates groundwater with respect to dissolved bicarbonate (HCO_3^-), carbonate (CO_3^{2-}) and aqueous carbon dioxide ($CO_{2\,(aq)}$). It is assumed that the current pH of the lake (~8.1) was maintained throughout the duration of calcite precipitation over the last 11,800 cal. yBP, and that HCO_3^- has therefore always been the dominant carbon species in this well-buffered carbonate system. $\delta^{13}C_{CaCO_3}$ values will be forced by changes to the carbon balance of the lake. Diefendorf et al. (2007) generated a model applicable to hard water lakes in limestone regions (Fig. 4.1). They illustrate how $\delta^{13}C_{CaCO_3}$ values generated by carbonate lakes are influenced by multiple carbon sources that contribute to the lake's carbon budget (Diefendorf et al., 2007). Generally, there are 4 dominant components making up lacustrine carbonate sediment: 1) inorganically precipitated carbonate; 2) photosynthetically-induced carbonate (bio-induced); 3) biogenic carbonate (debris from calcareous plants and animals; and, 4) allochthonous material derived from carbonate rocks in the lake's basin (Hren and Sheldon, 2012; Platt and Wright, 2009). The majority of the calcite in the UHL core is bio-induced calcite precipitated on the surface of the green algae *Chara corallina*.

4.1.1 Upper Hogarth Lake Carbon Cycle

Carbon inputs to UHL are similar those proposed by Diefendorf et al. (2007). The lake is an open system in exchange of CO_2 with the atmosphere during the ice-free period of each year. There are 3 significant sources of exogenous carbon: oxidized particulate organic carbon (POC), terrestrial particulate organic carbon (TPOC) and weathered carbon (WC) sourced from surrounding bedrock and the oxidation of organic matter (Diefendorf et al., 2007). $\delta^{13}C$ values of

dissolved inorganic carbon ($\delta^{13}C_{DIC}$) of carbonate lakes are primarily controlled by changes in the inorganic and organic carbon flux into the lake, primary productivity, organic matter (OM) burial, heterotrophic respiration, TPOC, calcite burial and dissolution, and CO_2 equilibration with the atmosphere (Diefendorf et al., 2007). The effects of calcite dissolution can be ignored

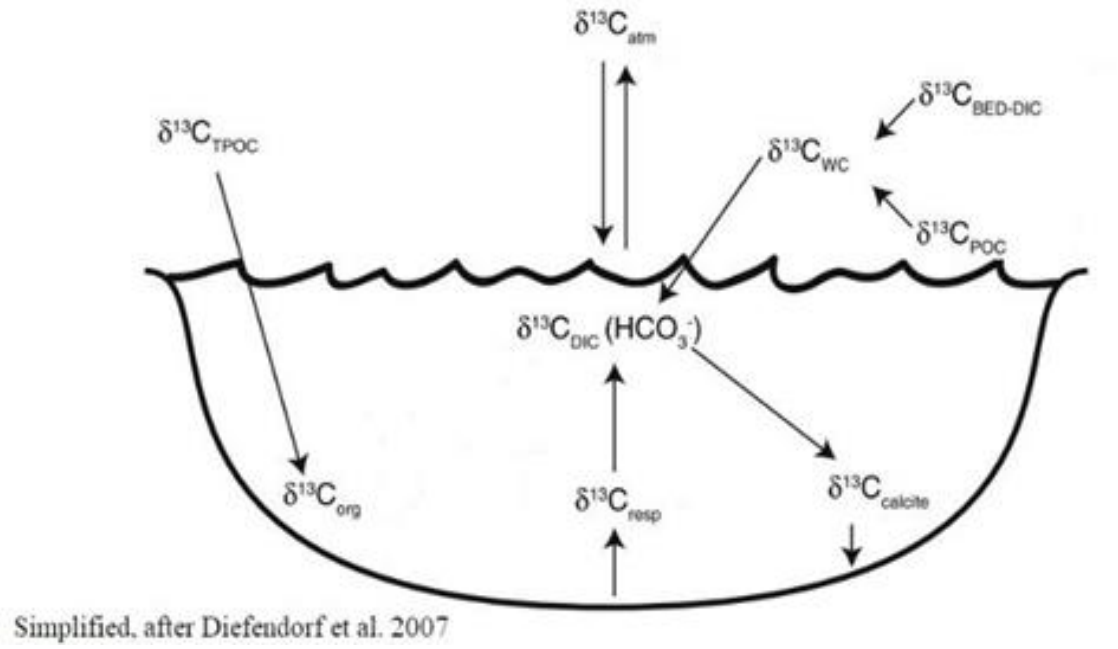

Figure 4.1. Carbon flux for a hardwater lake. TPOC: terrestrial particulate organic carbon; ORG: organic; RESP: respired; ATM: atmosphere; WC: weathered carbon; BED-DIC: dissolved inorganic carbon from bedrock; POC: particulate organic carbon, after Diefendorf et al., 2007.

because UHL was likely always saturated with respect to calcite. TPOC plays a minimal role as it is oxidized and therefore does not significantly influence $\delta^{13}C_{DIC}$ values. As UHL is (at present) an oligotrophic lake, heterotrophic respiration is not addressed in this study. Lake water $\delta^{13}C_{DIC}$ is influenced by the input of 2 primary external sources: terrestrial DIC, and oxidized POC (Diefendorf et al., 2007). The terrestrial-sourced DIC for UHL is introduced via rainfall, groundwater and snowmelt. Weathered inorganic carbon (WC) in the UHL water column is regulated by contributions from two isotopically distinct sources: 1) local limestone bedrock (BED-DIC) ($\delta^{13}C$ = ~ 0.5‰), and 2) CO_2 sourced from the oxidation of POC and/or DIC. Because the $\delta^{13}C$ value of the surrounding limestone bedrock remained constant through the Holocene, changes in $\delta^{13}C_{CaCO_3}$ must be forced by the other mechanisms. POC is derived from soil, terrestrial organic matter (plants), and decaying lake vegetation.

4.1.2 Plants

Plant carbon exhibits lower $\delta^{13}C$ values than atmospheric CO_2, because plant tissues discriminate against ^{13}C during photosynthesis of sugars (Bowling et al., 2008). This is due in part to the difference in diffusion rates of $^{12}CO_2$ and $^{13}CO_2$ into leaves during photosynthesis. Plants preferentially sequester $^{12}CO_2$ for photosynthesis. Modern atmospheric CO_2 has a $\delta^{13}C$ value between -8.5‰ VPDB (e.g., Patterson, 2017) and -8.0‰ VPDB (Bowling et al., 2008), about 1‰ lower than pre-industrial values. C_3 plants exhibit $\delta^{13}C$ values that can vary between -24‰ and -34‰ VPDB, while plants utilizing the C_4 photosynthetic pathway generally exhibit $\delta^{13}C$ values between -9‰ and -15‰ VPDB. Based on pollen studies (Luckman and Kearney, 1986; Macdonald, 1989; Mathewes and Heusser, 1980; Reasoner and Huber, 1999; Vance, 1986) and due to UHL's geographic location and elevation, it is assumed that C_3 woody plants were dominant for the duration of the Holocene while acknowledging the possibility of the propagation of C_4 grasses during warmer and drier times of higher tree lines. Vegetation-sourced organic matter as POC, is an important source of carbon to the lake carbon budget. Kinetic fractionation of $^{13}C/^{12}C$ in an open system results in the residual organic matter in the soil exhibiting higher $\delta^{13}C$ values (Wynn, 2007). C_3 plant dominated ecosystems may exhibit significant variability in $\delta^{13}C$ values of DIC, DOC, and POC supplied to soils (Bowling et al., 2008). It is this variation, along with the plant's response to soil moisture availability that will force UHL $\delta^{13}C_{CaCO_3}$ values. Terrestrial C_3 plants systematically react to moisture availability by physically controlling CO_2 diffusion through their stomates. Leaf intercellular air is saturated with water vapor, resulting in higher water vapor pressure inside the leaf than the comparatively dry extracellular air. C_3 plants (and plants in general) discriminate against ^{13}C because breaking $^{13}CO_2$ bonds is energetically costlier for the plant. Plants will leave their stomates open more frequently, allowing for increased diffusion of ^{12}C into the intracellular space. During periods of low humidity, stomates are open less frequently to conserve moisture by limiting transpiration. During limited 'open-stomate' periods, the plant is unable to preferentially sequester sufficient $^{12}CO_2$ and must utilize more $^{13}CO_2$. Thus, photosynthetic fractionation generates a $\delta^{13}C$ value in the plant's tissue that is transmitted to the organic matter (POC) of the leaf and twig litter before entering the lake carbon cycle. At present, Upper Hogarth Lake lies in a coniferous forest amongst limestone bedrock and- carbonate rich soil and gravel. The record will illustrate the transition from barren glacial till, to herbs and shrubs, to its current forested state. Therefore,

carbon isotope variability is forced by changes in local productivity, vegetative succession within the lake catchment and changes in humidity and soil moisture.

4.2 Results and Interpretation

This study presents a record of $\delta^{13}C$ values of carbon archived by lacustrine calcite that dates back approximately 12,000 years. Over 750 data from the 3.6m core provide proxy evidence for an evolving subalpine basin; from a newly formed, muddy lake to a clear water marl lake. $\delta^{13}C$ values (presented here as $\delta^{13}C_{CaCO_3}$) range from -4.1‰ to +3.2‰ VPDB (Fig. 4.2), demonstrating significant variability through the Holocene. These data represent the vegetative history of the region, changes to the lake carbon budget, and variation in humidity and soil moisture. The $\delta^{13}C_{CaCO_3}$ record is, in part, reflective of the transition of a newly formed kettle lake surrounded by glacially scoured Carboniferous limestone to its current state of productive marl lake surrounded by coniferous forest.

As described in the "Methods" section; the changes in lithology and constraints of the age model restricts the ability to accurately ascribe any time-precise environmental forcing of data beyond 11,800 cal. yBP. However, based on the sediment and on the $\delta^{13}C$ values, as described in the core description section of this paper; this gyttja represents an evolving lake bottom with increased organic input.

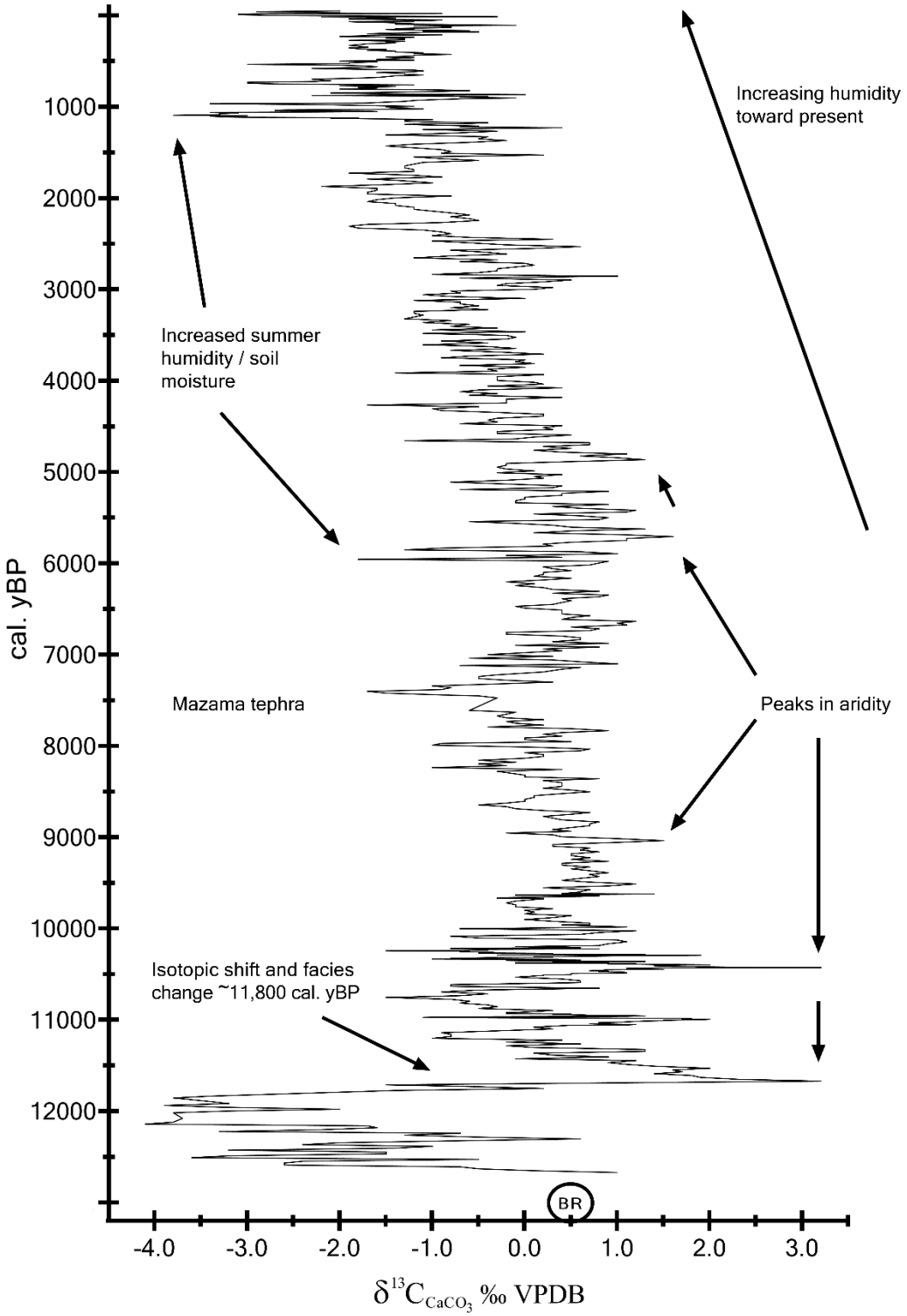

Figure 4.2. $\delta^{13}C_{CaCO_3}$ values of Upper Hogarth Lake marl. Lower values indicate increased humidity and soil moisture while higher values indicate increased aridity. "BR" indicates value of surrounding bedrock ($\delta^{13}C$ = 0.5‰ VPDB).

4.2.1 Termination of the Pleistocene

Beginning at the base of the 3.6m core, $\delta^{13}C_{CaCO_3}$ values of the basal diamict display values of ~0.2‰ VPDB, consistent with the average value of the surrounding bedrock (0.5‰ VPDB, *n*=9) (Fig. 4.2). The values of the overlying mud exhibit a range in values. $\delta^{13}C_{CaCO_3}$ values for the end-Pleistocene sediment are interpreted to represent inorganic sediment associated with clastic input and the expansion of alpine glaciers (Crowfoot Advance/Younger Dryas event) (e.g. Reasoner and Huber, 1999). $\delta^{13}C_{CaCO_3}$ values remain at ~0.2‰ VPDB, consistent with local bedrock as the dominant source of carbon, with little contribution of terrestrial vegetation, a hypothesis supported by low pollen counts in other studies (Macdonald, 1989; Reasoner and Huber, 1999). $\delta^{13}C_{CaCO_3}$ values increase upward within the mud section (Zone IV, Fig. 2.2). As the core becomes more laminar beginning with a distinct black lamina (A in Fig. 4.4) at 2.88m (>12,000 cal. yBP), the sediment exhibits low (-2.5‰) $\delta^{13}C_{CaCO_3}$ values. From post-glaciation to ~11,700 cal. yBP, the recently deglaciated terrain was sparsely vegetated (Macdonald, 1989; Reasoner and Huber, 1999). At a nearby lake, a thin, discontinuous shrub-herb vegetative cover dominated by *Artemesia, Salix,* and *Juniperus* was inferred by palynology for the Pleistocene-Holocene transition (Macdonald, 1981; Reasoner and Huber, 1999). This study supports those findings, as several pollen sacs with morphological characteristics consistent with *Juniperus* were recovered from the sediment at a depth of 2.70m or >12,000 cal. yBP.

4.2.2 Early Holocene

The Early Holocene (~11,500 – 9,500 cal. yBP) was a period of higher-than-present treelines and warmer-than-present summer temperatures (Luckman and Kearney, 1986; Mathewes and Heusser, 1980; Reasoner and Huber, 1999), coinciding with peak summer insolation (Berger and Loutre, 1991; Berger, 1979; Pendleton et al., 2017). For the UHL record, the sudden onset of the Holocene is marked by an abrupt change in lithology (B in Fig. 4.4) and a large excursion in the $\delta^{13}C_{CaCO_3}$ record (Fig. 4.2). This occurs at a depth of 2.63m correlating to a calibrated age of ~11,800 cal. yBP. A 7‰ increase in $\delta^{13}C_{CaCO_3}$ occurs from 11,900 – 11,700 cal. yBP. This may have been caused by a change in the carbon flux with a shift to lower POC contribution to the lake, or by desiccation of the surrounding soil. Organic carbon recovered from marl lakes exhibits $\delta^{13}C$ values ~15-20‰ lower than DIC (Drummond et al., 1995). Anoxic bottom waters

are often accompanied by increased organic carbon burial that would result in lower $\delta^{13}C_{CaCO_3}$ values. The isotopic shift is accompanied by a change from gyttja to cream-colored marl that may be explained by changing lake morphology (marl bench progradation). Borzenkova et al. (2015) observed a similar facies shift ~11,600 cal. yBP in their record from a similar lake in Poland. They explained it as a shift from clastic-detrital dominant deposition to autochthonous biochemical (bio-induced) calcite as a result of climate amelioration. Marl bench progradation means that the depositional surface became shallower and likely more oxygenated, such that organic carbon would be increasingly oxidized, increasing the influence of DIC over POC in the carbon budget. A regional increase in aridity may have forced this change. A decrease in soil moisture would have resulted in proliferation of drought-tolerant pioneer species. At a nearby lake, Reasoner et al. (1999) found that around 11,700 cal. yBP there were significant changes in the paleobotanical record concomitant with the abrupt onset of organic sedimentation, interpreted as the establishment of an open *Pinus* – dominated forest (Reasoner and Huber, 1999). They observed a sharp increase in arboreal pollen and a shift from clastic to organic sedimentation around 11,700 cal. yBP at their study site, representing the stabilization of the landscape and increase in forest vegetation in the area (Reasoner and Huber, 1999). This rapid expansion of forest vegetation is ubiquitous in the Canadian Rocky Mountains and adjacent foothills during the Early Holocene (Macdonald, 1989; Reasoner and Huber, 1999; Reasoner and Jodry, 2000; Vance, 1986). Charophyte calcite can confidently be associated with cream-colored marl deposition commencing at 2.63m (11,800 cal. yBP) based on calcified *Chara sp.* stems found

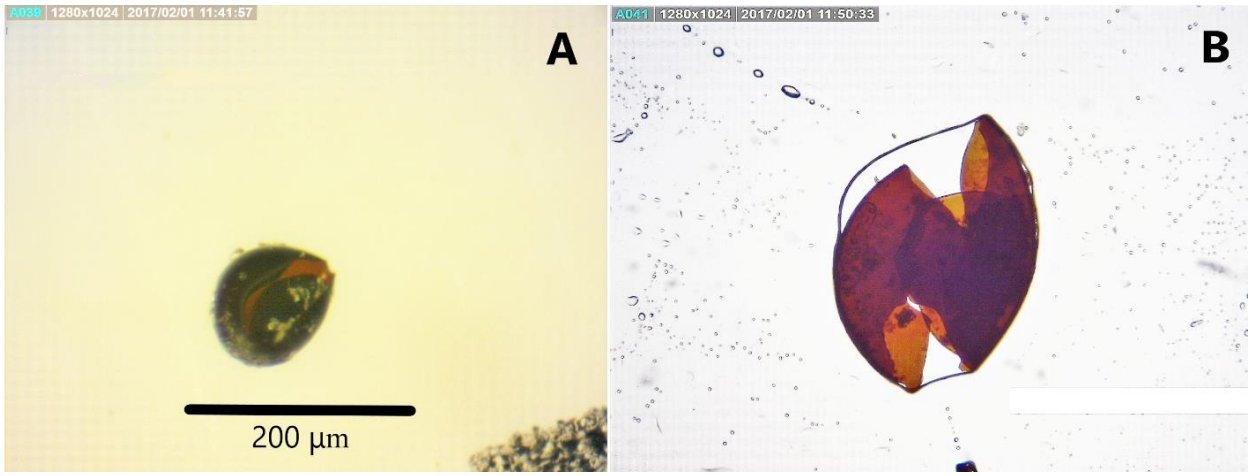

Figure 4.3. A *and* B*: Suspected Juniperus sp. pollen sac recovered from Upper Hogarth Lake core at ~2.7m (~12,000 cal. yBP).*

Figure 4.4. Upper Hogarth Lake core (2.56m-3.05m) illustrating changes in lithology. A*: initial appearance of laminar features (>12,000 cal. yBP).* B*: onset of Holocene Epoch (11,700 cal. yBP).*

in the brown muds immediately below (zone 1, Fig. 2.2 and B in Fig. 4.4). Following the brown sediment transition, cream colored marl deposition begins and persists for the remainder of the core. Cream-colored marl associated with the period between 11,800 and 10,200 cal. yBP does not appear as uniformly colored as the overlying younger marl. It has more darker laminae distributed within, along with some darker colored lenticular spotting (Fig. 4.5). A possible explanation for this could be that bacteria and algae colonized the basin in the littoral zone, as microbial mats and oncolites. These microbialites now appear as darker marl lamina and lenses amongst the cream-colored marl.

Figure 4.5. Microbialites (dark lenses amid cream-colored marl) in Upper Hogarth Lake Core (2.39m-2.63m). Way-up is to the left.

4.2.3 Isotopic Covariance

Between 11,500 and 10,400 cal. yBP there is significant ($R^2 = 0.42$) covariance (Fig. 4.6) in the $\delta^{18}O_{CaCO_3}$ and $\delta^{13}C_{CaCO_3}$ values. Drummond et al. (1995) documented that isotopic covariance in a hydrologically open temperate region marl lake is indicative of a shift in climate. There are significant positive (negative) excursions in the $\delta^{18}O_{CaCO_3}$ and $\delta^{13}C_{CaCO_3}$ records at 11,000 (10,700) and 10,400 (10,200) cal. yBP. $\delta^{13}C_{DIC}$ values of lake water are strongly dependent upon the duration and magnitude of summer thermal and redox stratification (Drummond et al., 1995). A generally warmer climate with a longer summer growing season means that UHL would remain thermally stratified for more of the year. This would also mean that summer rain, with higher $\delta^{18}O_{H_2O}$ values, was a larger contributor to the lake water budget, observed as higher $\delta^{18}O_{CaCO_3}$ values. Longer growing seasons and warmer summers increase evaporation, which would also force higher $\delta^{18}O_{\text{lake water}}$ values. A longer growing season allows for more photosynthetic modification (plants using relatively more $^{12}CO_2$) of the carbon in the lake (Drummond et al., 1995), also forcing higher $\delta^{13}C_{CaCO_3}$ values. Longer, warmer and drier

summers may have resulted in an increase in the proportion of C_4/C_3 plants in the lake watershed. Increased contribution of C_4 plant organic carbon to the carbon pool of the basin would also force higher $\delta^{13}C_{CaCO_3}$ values.

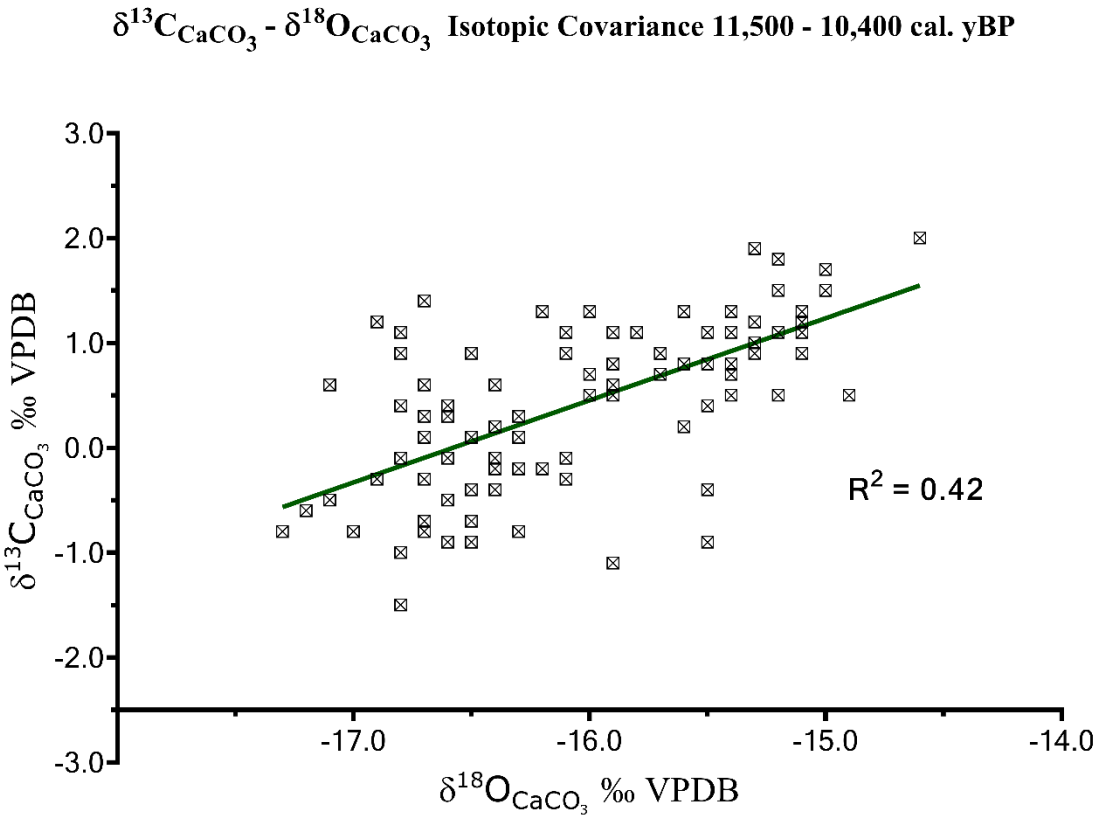

Figure 4.6. Isotopic covariance of UHL marl for 11,500 – 10,400 cal. yBP. $\delta^{13}C_{CaCO_3}$ vs. $\delta^{18}O_{CaCO_3}$ values (n=95). This covariation is likely related to a longer growing season with an increase in the summer/winter precipitation ratio.

Covariant negative excursions may be explained by a transition to a cooler, wetter climate with higher proportions of snowfall. More colder months means longer periods of winter stratification and a buildup of respired CO_2 from organic carbon in the sediment, resulting in a carbon pool with lower $\delta^{13}C$ values and lower $\delta^{13}C_{CaCO_3}$ values (Drummond et al., 1995). Following ~10,200 cal. yBP a decrease in variability is observed in the $\delta^{13}C_{CaCO_3}$ record, along with a decoupling from the variability of $\delta^{18}O_{CaCO_3}$. This may be attributed to the rise in sea-level and flooding of Beringia (described in the $\delta^{18}O$ section), along with a shift in atmospheric circulation to more closely resemble the modern.

4.2.4 Early to Mid-Holocene

From ~9,500 – 4,500 cal. yBP there was an increase in regional aridity. Low humidity results in decreased discrimination against $^{13}CO_2$ and higher $\delta^{13}C_{TPOC}$ values entering the lake carbon pool. Reasoner and Huber (1999) found an increase in macroscopic charcoal after 10,200 cal. yBP with peak values between 7,600 and 6,400 cal. yBP. When combined with their pollen record, it is indicative of drier climatic conditions conducive to more frequent fires. Increases in the abundance of *Pinus* relative to *Picea* and *Abies* during the Mid-Holocene also suggests an increased fire frequency and a warmer, drier climate (Macdonald, 1981). Following deposition of the Mazama tephra ~7,600 cal. yBP, $\delta^{13}C_{CaCO_3}$ values peak during the Mid-Holocene from ~7,000 – 4,500 cal. yBP, marking the driest period of the UHL record. Aridity likely peaked around 6,700 and 4,800 cal. yBP (Fig. 4.2), suggested by positive excursions in $\delta^{18}O_{CaCO_3}$ and $\delta^{13}C_{CaCO_3}$ values. In the southwestern Yukon during the Mid-Holocene, a similar carbonate lake recorded water levels 5-6m below modern (Anderson et al., 2005). Paleoecological and diatom studies in subalpine Alberta suggest the Mid-Holocene was a period of increased temperatures, higher alpine tree lines, and spreading of grasslands into the valleys and foothills (Heinrichs et al., 2001; Hickman and Reasoner, 1998; Macdonald, 1989).

4.2.5 Neoglacial – Present

In the Northern Hemisphere, the Neoglacial marked a transition from warm and dry to cool and wet. The "general consensus" is that this transition occurred between 5,700 and 3,200 cal. yBP (Reasoner and Huber, 1999). The onset of wetter conditions can be observed as a steady decrease in $\delta^{13}C_{CaCO_3}$ values beginning ~4,500 cal. yBP. A similar carbonate lake in Yukon saw water levels rise from Mid-Holocene levels to levels greater than the present between 4,000 and 2,000 cal. yBP (Anderson et al., 2005). The steady decrease in $\delta^{13}C_{CaCO_3}$ is interrupted by a 600-year period of higher values centered around 3,100 – 2,500 cal. yBP. This period is coincident with reported glacier expansion in the Yukon from 3300 – 2400 cal. yBP (Denton and Karlen, 1973). A period of anomalously lower $\delta^{13}C_{CaCO_3}$ values is observed 2,400 – 1,600 cal. yBP, suggesting increased humidity and soil moisture. When combined with a relative peak in $\delta^{18}O_{CaCO_3}$, it suggests an increase in summer precipitation. This period is concurrent with the Roman Warm Period (RWP) recorded in Europe (Bianchi and McCave, 1999). Values then fluctuate significantly for the next 1500 years indicating a period of moisture variability where

values first increase by 2‰ then decrease by over 3.5‰ at ~1000 cal. yBP. $\delta^{13}C_{CaCO_3}$ values remain low from 1100 - 960 cal. yBP, suggesting increased humidity, coeval with the Medieval Climate Anomaly (MCA) (Mann et al., 2009). From 960 – 800 cal. yBP there is a positive 3‰ excursion of $\delta^{13}C_{CaCO_3}$ and 1‰ positive excursion in $\delta^{18}O_{CaCO_3}$ values, suggesting a time of increased aridity. This arid period is coeval with the reported collapse of Mayan civilization ~850 C.E. (Alley, 2004). Values then fluctuate markedly until present, indicative of century-scale variability in soil moisture/relative humidity coeval with the onset of the Little Ice Age (LIA) (e.g., Kreutz et al., 1997; Reyes et al., 2006) and the subsequent Modern Warm Period. The increase in the most recent $\delta^{13}C_{CaCO_3}$ values may be ascribed to increased summer humidity and soil moisture as the result of increased melting of the alpine snowpack. This increase in melting is the result of warming atmospheric temperatures in Western Canada since 1950 CE (DeBeer et al., 2016; Thériault et al., 2018).

CHAPTER 5 OXYGEN ISOTOPE RECORD OF UPPER HOGARTH LAKE MARL

5.1 $\delta^{18}O$ Values of Upper Hogarth Lake Marl

$\delta^{18}O_{CaCO_3}$ values of calcium carbonate marl are reflective of three variables: 1) water temperature at the time of precipitation; 2) $\delta^{18}O_{lake\ water}$; and, 3) mechanism of precipitation. The mechanism of precipitation for the bulk of UHL marl is bio-induced, extracellular precipitation of calcite on the surface of macroscopic algae (*Chara sp.*). This is assumed to have been the dominant process for the entirety of the UHL Holocene record. Calcite precipitates as a by-product of photosynthesis by *Chara sp.* (Mcconnaughey et al., 1994, 1991), thus, the values recorded will reflect the $\delta^{18}O_{lake\ water}$ and water temperature during the charophyte growing season. The temperature of the lake water is representative of atmospheric temperature that in turn varies in response to the position of the northern Polar Front Jet Stream, oceanic heat transport, sea surface temperatures, insolation, surface albedo, and other variability in atmospheric circulation. $\delta^{18}O_{lake\ water}$ values will vary according to the hydrology of the basin and the value of the recharge water (precipitation and ground water).

5.1.1 Hydrology

In larger lakes, long residence times more substantially moderate the influence of a climatic perturbation relative to a smaller lake (Steinman and Abbott, 2013). The isotopic response to climatic forcing is greater in smaller lakes than volumetrically larger lakes with longer residence times. UHL is a small, hydrologically open basin with a short residence time due to spring/summer outflow to Middle Hogarth Lake and exchange with the underlying alluvial fan aquifer. The small basin size and shorter residence time are favorable for high-resolution isotope studies.

5.1.2 $\delta^{18}O$ of UHL Precipitation and Lake Water

$\delta^{18}O_{lake\ water}$ is reflective of the annual weighted average $\delta^{18}O$ value of local precipitation ($\delta^{18}O_{PPT}$). Peng et al. (2004) conducted a 10-year (1992-2001) study of amount-weighted average isotope values of precipitation at Calgary, Alberta. They found the annual average value for the $\delta^{18}O_{H2O}$ of Calgary precipitation to be -17.9‰ VSMOW. The annual weighted average value for $\delta^{18}O_{PPT}$ will vary based on the dominant seasonality of the precipitation (i.e. winter vs. summer), with snow exhibiting lower values (~ -26‰ VSMOW; Moran et al., 2007; Peng et al., 2004) and summer exhibiting higher values (~ -16‰ VSMOW; Peng et al., 2004). The value of $\delta^{18}O_{PPT}$

varies with atmospheric temperature seasonality) by 0.6‰/°C globally (e.g. Dansgaard, 1964; Rozanski et al., 1992). The relationship for nearby Calgary, Alberta was determined to be 0.44‰/°C (Peng et al., 2004). At present, the Hogarth Lakes region receives more snow (SWE) than rain annually (Bow River Basin Council, 2010; Government of Alberta, n.d.). Changes in the dominant phase of meteoric water (snow vs. rain) for the UHL region will be recorded in $\delta^{18}O_{CaCO_3}$ values of UHL marl.

5.1.3 Lake Water (Atmospheric) Temperature

The temperature of UHL water will reflect atmospheric temperature with some attenuation due to the thermal inertia of water. The principal control on Alberta temperature is the dominant air mass (Chapter 1). A dominant Continental Polar (cP) air mass will force lower temperatures, while a dominant Maritime Pacific (mP) or Maritime Tropical (mT) air mass would result in higher temperatures. The dominant air mass is dependent on the position of the northern Polar Front Jet Stream. The position of the Polar Front Jet Stream depends on the season and a combination of complex atmospheric and meteorological variables, such as Pacific sea surface temperatures, and the position of semi-permanent high- and low-pressure features like the Pacific High and Aleutian Low. Prolonged expansion of the Circumpolar Vortex (CPV) towards lower latitudes results in colder polar air remaining over the UHL region for longer periods.

If the UHL record is interpreted as reflecting only Holocene temperature variation (i.e. $\delta^{18}O_{lake\ water}$ remained constant), it requires a variation in mean annual temperature of ~20 °C over the last ~12,000 years. This is unlikely because such temperature variability is not observed in any other North American Holocene paleoclimate records. Following the end of the Younger Dryas (~11,500 cal. yBP), Holocene temperatures in North America are reported to have varied by 1-4 °C (Renssen et al., 2012; Viau et al., 2006). $\delta^{18}O_{CaCO_3}$ values fluctuate significantly at decadal-scale through the Holocene, indicating that temperature is not the primary driver of variation. While temperature may have an overprinting effect on the record, changes in atmospheric circulation and the dominant seasonality of precipitation, and subsequently, $\delta^{18}O_{lake\ water}$ will be the primary drivers of UHL $\delta^{18}O_{CaCO_3}$ variability.

5.1.4 Seasonality of Precipitation

The Hogarth Lakes are part of the Upper Bow River sub-basin. A study in 2010 estimated that 80% of the sub-basin's water is sourced from snowmelt (Bow River Basin Council, 2010).

In environments where snowfall accounts for the majority of the annual precipitation budget, snowmelt is likely to have the strongest influence on isotope values retained in proxy archives (Anderson et al., 2016). During periods of increased snowfall relative to summer rain $\delta^{18}O_{CaCO_3}$ values should be forced lower. During periods of increased summer rain relative to winter snow, $\delta^{18}O_{CaCO_3}$ values should increase. Snow in the UHL region is most often sourced from the Pacific Ocean (Moran et al., 2007; Van Der Ent and Savenije, 2013) as the result of zonal atmospheric flow over mid-latitude North America. Summer rain may originate from more southerly sources like the Gulf of Mexico or evapotranspiration over the Great Plains (Milrad et al., 2015; Moran et al., 2007) due to the more meridional atmospheric flow pattern common in the summer season. The dominance of snow vs. rain as lake water recharge will be reflected in the $\delta^{18}O_{CaCO_3}$ values of UHL marl.

5.2 Results and Interpretation

$\delta^{18}O_{CaCO_3}$ values provide a proxy record for variation in the dominant form of precipitation for UHL through the Holocene with water temperature overprinting. Values vary significantly (Fig. 5.1) over the Holocene, from -18.8‰ VPDB in the Mid-Holocene to -14.6‰ VPDB in the Early Holocene. $\delta^{18}O_{CaCO_3}$ values of UHL marl will have changed as the result of variation in $\delta^{18}O_{lake\ water}$ values and summer water temperature. Changes in the duration or magnitude of seasonal climate patterns can have a profound effect on the average $\delta^{18}O_{H2O}$ value of precipitation, and consequently, lake water (Drummond et al., 1995).

5.2.1 Pleistocene – Holocene Transition

The Pleistocene – Holocene transition is characterized by significant changes in North American atmospheric circulation and climate. The Laurentide and Cordilleran ice sheets were retreating to the north, followed by the mean position of the Circumpolar Vortex. The sediment corresponding to the period (>11,800 cal. yBP) consists of sand, mud, and gravel (Chapter 1). $\delta^{18}O$ values of the basal diamict of -8.6‰ VPDB (not shown) are consistent with average values of local bedrock outcrops (-8.5‰ VPDB, *n=8; BR in Fig. 5.1*). The >12,000 cal. yBP mud (zone IV, Fig. 2.2) has a $\delta^{18}O_{CaCO_3}$ value of ~-9.4‰ VPDB, indicating that a dominant source of carbonate was local bedrock. The onset of the Holocene (~11,500 cal. yBP) follows the commencement of cream-colored marl deposition dated at 11,800 cal. yBP by the age model.

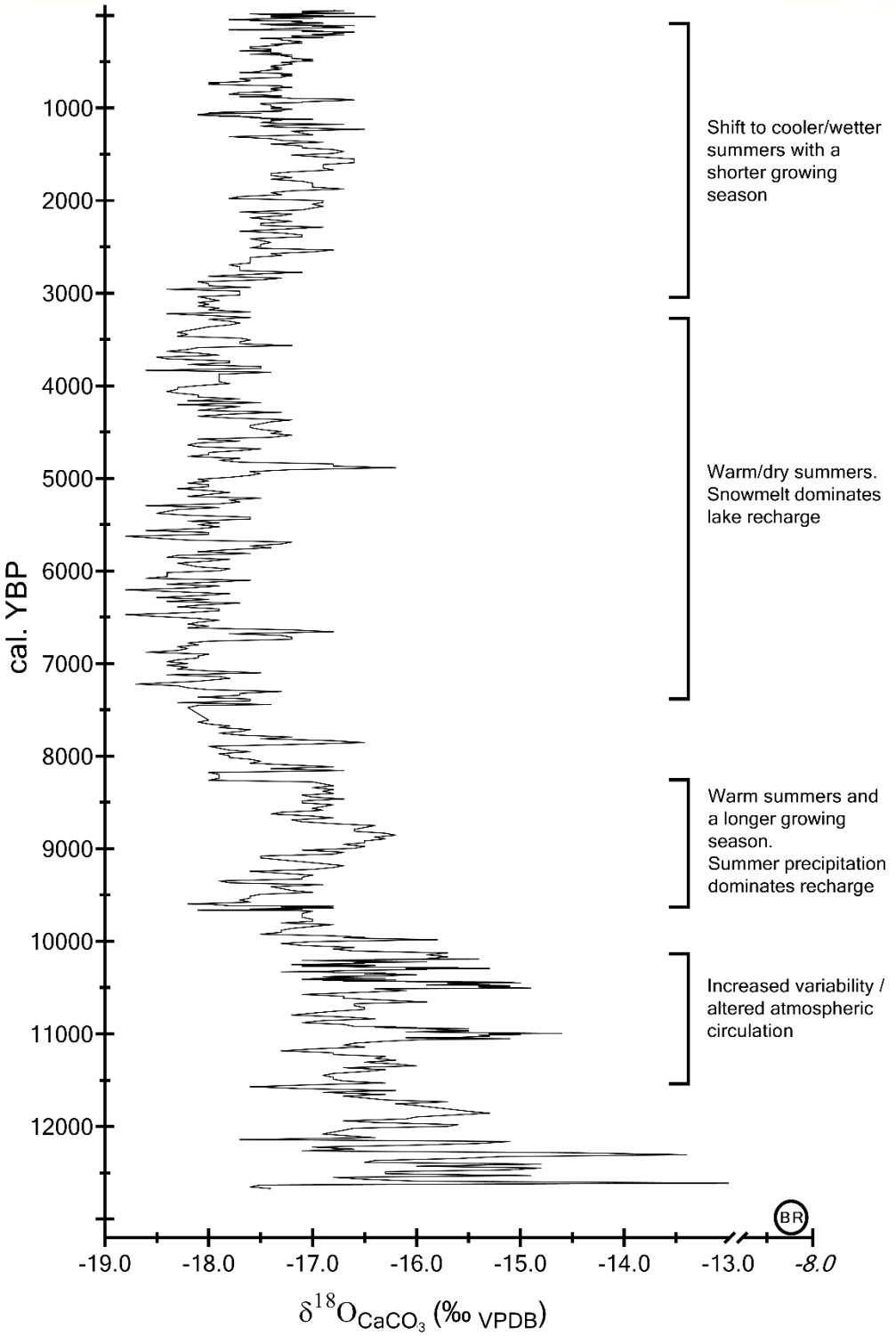

Figure 5.1. $\delta^{18}O_{CaCO_3}$ values of Upper Hogarth Lake marl. Increased variability in the Early Holocene (11,500-7,500 cal. yBP), warm and dry Mid-Holocene (7,500-3,000 cal. yBP), and cool and wet Neoglacial (3,000 cal. yBP – Modern). "BR" indicates value of local bedrock ($\delta^{18}O$ = -8.6‰ VPDB)

5.2.2 Early Holocene

$\delta^{18}O_{CaCO_3}$ values from the Early Holocene (11,500 – 10,000 cal. yBP) are generally higher with greater variability than the Mid and Late Holocene. Temperatures were likely warmer, due to peak summer insolation (Berger and Loutre, 1991). The $\delta^{13}C_{CaCO_3}$ record suggests summers that alternated between wet and dry and winters were likely shorter with less snow, indicated by the generally higher $\delta^{18}O_{CaCO_3}$ values. This may have been a time of unstable precipitation patterns in the region, associated with an atmospheric circulation pattern that has not been observed in modern times. I believe the cause of this circulation pattern is related to a subaerially exposed Beringia (Bering Strait).

Atmospheric circulation and Northern Hemisphere climate is closely linked to sea surface temperatures and Atlantic Ocean heat transport (Hu et al., 2012; Wanner et al., 2011). When the Bering Land Bridge was subaerially exposed, the Bering Strait was closed, sea water was not exchanged between the warmer Pacific and the colder Arctic Ocean and North Atlantic Ocean. During the Early Holocene, proglacial Lake Agassiz was discharging large amounts of freshwater into the North Atlantic and Arctic Oceans. This freshwater is believed to have disrupted/decreased thermohaline circulation and heat transport by the Atlantic Ocean (Fisher et al., 2002b; Hu et al., 2010; Teller et al., 2002). Freshwater anomalies in the North Atlantic during glacial periods resulted in large-amplitude climate oscillations (De Boer and Nof, 2004). It has been proposed that the Bering Strait acts as an "exhaust valve" for the North Atlantic (via the Arctic Ocean) to more rapidly equalize these freshwater anomalies (De Boer and Nof, 2004; Hu et al., 2010). With the Bering Strait closed prior to ~10,400 cal. yBP (De Boer and Nof, 2004), the UHL $\delta^{18}O_{CaCO_3}$ record displays larger amplitude variability, relative to the period following the flooding of Beringia. Increased (~3.0‰) variability in the UHL $\delta^{18}O_{CaCO_3}$ record prior to 10,200 cal. yBP suggests more extreme climatic variation and/or atmospheric circulation changes not observed in the Mid or Late Holocene.

Following the flooding of Beringia ~10,400 cal. yBP, the large-amplitude variation in the $\delta^{18}O_{CaCO_3}$ record decreased, and atmospheric circulation likely assumed patterns more similar to the present day. It has been suggested that warmer temperatures may have caused the complete ablation of the nearby Robertson Glacier shortly after the onset of the Holocene epoch (Beierle et al., 2003). Peat and pollen studies from central Beringia suggest conditions were warmer than present ~9,700 cal. yBP (Kaufman et al., 2004; Vartanyan, 1997).

From 9,500 – 9,000 cal. yBP, $\delta^{18}O_{CaCO_3}$ values increase, suggesting summer rain was becoming a more significant source of water recharge for UHL. As alpine glaciers were ablated, and the continental ice margin retreated, meltwater and clastic influx to the basin reached a minimum. Complete ablation of local alpine glaciers has been suggested for this period (Beierle and Smith, 1998; Beierle, 1997; Beierle et al., 2003; Leonard and Reasoner, 1999; Reasoner and Hickman, 1989). Peak $\delta^{18}O_{CaCO_3}$ values ~9,000 cal. yBP suggests a predominantly summer moisture source for UHL with higher $\delta^{18}O_{PPT}$ values. Some studies suggest an earlier onset of the Holocene Thermal Maximum in western Canada, relative to eastern Canada (Clague et al., 1992; Kaufman et al., 2004; Luckman and Kearney, 1986; Mathewes and Heusser, 1980; Reasoner and Huber, 1999; Renssen et al., 2012, 2009). The Holocene Thermal Maximum (HTM) was a relatively warm climatic phase between 11,000 and 5,000 years ago, depending on the proxy record (Renssen et al., 2012). It is most clearly recorded in the mid to high latitudes of the Northern Hemisphere (Renssen et al., 2009).

$\delta^{18}O_{CaCO_3}$ values decrease from 9,000 cal. yBP to their lowest around 7,250 cal. yBP. This decrease suggests a shift from summer rain to snow as the dominant source of lake water. This may have been the result of a shift in atmospheric circulation, whereby zonal atmospheric circulation patterns were more frequent than meridional, limiting any easterly or southerly sources of summer rain. Warmer temperatures, reported by other proxies, may have resulted in the complete melting of all annual snowfall in the region every summer (Kaufman et al., 2004; Leonard and Reasoner, 1999; Luckman and Kearney, 1986; Reasoner and Huber, 1999). The increased amount of snowmelt would also force the lower $\delta^{18}O_{CaCO_3}$ values observed during the beginning of the Mid-Holocene. A decrease in summer precipitation is supported by higher $\delta^{13}C_{CaCO_3}$ values of UHL marl, indicative of arid summer conditions. A large negative excursion in the UHL $\delta^{18}O_{CaCO_3}$ record may be related to the commonly recorded 8.2 ka climate event (Alley et al., 1997) associated with a final outburst of 163,000 km^3 of freshwater from Lake Agassiz (Alley et al., 1997; Teller et al., 2002).

5.2.3 Mid-Holocene

UHL water recharge during the he Mid-Holocene was dominated by snow melt, as indicated by the lowest $\delta^{18}O_{CaCO_3}$ values of the record. The dominance of snow melt was accompanied by arid summers with decreased meridional summer moisture transport, a theory

supported by higher $\delta^{13}C_{CaCO_3}$ values (increased aridity) of UHL marl. Palynological studies in SW Alberta and SE British Columbia suggest increased forest fire frequency and severity during the Mid-Holocene (Heinrichs et al., 2001; Macdonald, 1987). Paleoecological and diatom studies in subalpine Alberta suggest the Mid-Holocene was a period of higher alpine tree lines and increased grassland in the valleys and foothills (Heinrichs et al., 2001; Hickman and Reasoner, 1998; Macdonald, 1989). Positive excursions at 6,600 and 4,800 cal. yBP likely represent decadal scale periods of increased evaporation of lake water, supported by coeval positive excursions in the $\delta^{13}C_{CaCO_3}$ (decrease in humidity) record.

5.2.4 Neoglacial – Present

The transition from a warm and dry Mid-Holocene to the cool and wet Neoglacial occurred sometime between 5,700 and 3,200 cal. yBP. An increase in summer humidity begins as early as 4,600 cal. yBP at UHL, indicated by the commencement of decreasing $\delta^{13}C_{CaCO_3}$ values. A remarkable shift in the trend of $\delta^{18}O_{CaCO_3}$ values doesn't occur until around 3,000 cal. yBP, where low Mid-Holocene values gradually become more positive and peak (relative to Late Holocene values) around 1,500 cal. yBP. The increase in summer humidity (decrease in $\delta^{13}C_{CaCO_3}$ values) may be attributed to increased meridional transport of summer moisture, while warmer temperatures continued to melt the aggregated winter snowfall every summer – keeping $\delta^{18}O_{CaCO_3}$ values lower. It wasn't until 3,000 cal. yBP that temperatures cooled, allowing the expansion of glaciers and the persistent of year-round alpine snow, which shifted the water balance of the lake to less snowmelt and more summer rain, thereby increasing $\delta^{18}O_{lake\ water}$ and subsequently, $\delta^{18}O_{CaCO_3}$ values. $\delta^{18}O_{CaCO_3}$ variability from 1,500 cal. yBP to present remained less than ~1.5‰, with positive and negative excursions occurring at the centennial and sub-centennial scale, indicating short-lived changes to the water balance of the lake. An increase in variability in the most recent $\delta^{18}O_{CaCO_3}$ values is indicative of rapid changes in the source water to the lake. This may be explained by periods of increased summer storms paired with periods of increased melting of the alpine snowpack due to warming Western Canadian atmospheric temperatures (DeBeer et al., 2016; Thériault et al., 2018).

CHAPTER 6 CONCLUSIONS

6.1 Conclusions

Over 750 samples were recovered from the 3.6-meter long lake Upper Hogarth Lake sediment core. $\delta^{13}C_{CaCO_3}$ and $\delta^{18}O_{CaCO_3}$ values of the lacustrine marl provide a 12,000-year record of environmental variability in a subalpine Rocky Mountain valley. $\delta^{13}C_{CaCO_3}$ values of UHL marl represent changes in Holocene humidity and soil moisture as reflected in the TPOC contributed to the UHL carbon budget from plant tissue. $\delta^{18}O_{CaCO_3}$ values of UHL marl represent the dominant seasonality of precipitation in the region with overprinting by temperature and aridity.

The UHL $\delta^{13}C_{CaCO_3}$ record illustrates the transition of a newly formed subalpine lake surrounded by barren limestone and glacial till to a productive lake surrounded by coniferous forest. The Pleistocene-Holocene transition is marked by a large shift in $\delta^{13}C_{CaCO_3}$ values as surrounding soils dried, humidity decreased, and the dominant source of carbonate shifted to bio-induced calcite (marl). The Early Holocene (11,700 – 9,500 cal. yBP) is characterized by large centennial-scale variability in the $\delta^{13}C_{CaCO_3}$ record, indicative of impactful variation in regional humidity. Large positive excursions suggest increases in aridity in the region while lower values signify more humid conditions. The Mid-Holocene (9,500 – 4,500 cal. yBP.) was a period of warm and arid summers, suggested by predominantly high $\delta^{13}C_{CaCO_3}$ values, with negative excursions at 7,500 cal. yBP (following Mazama tephra deposition) and 5,900 cal. yBP. (unknown cause). The 5,900 cal. yBP negative excursion may have been a 100-200-year period of increased summer moisture. The onset of more humid summers begins ~4,500 cal. yBP, indicated by decreasing $\delta^{13}C_{CaCO_3}$ values, interrupted by an 800-year dry period from 3,200 – 2,400 cal. yBP. $\delta^{13}C_{CaCO_3}$ values then continue to decrease from 2,400 cal. yBP to present, in agreement with Neoglacial cooling and increasing humidity.

$\delta^{18}O_{CaCO_3}$ values of UHL marl provide proxy evidence of Holocene precipitation variability with respect to lake water recharge. $\delta^{18}O_{CaCO_3}$ values suggest warm summers with longer growing seasons and increased rain during the Early Holocene. Higher $\delta^{18}O_{CaCO_3}$ values indicate higher $\delta^{18}O_{lake\ water}$ values, produced from increased rainfall relative to snow. Rain dominated lake recharge persists until ~7,700 cal. yBP, when summers remained warm, but

humidity decreased (higher $\delta^{13}C_{CaCO_3}$). The $\delta^{18}O_{CaCO_3}$ values from 7,700 to 3,000 cal. yBP suggest an increase in snowmelt relative to summer rain as the dominant source of lake water. The lower $\delta^{18}O_{CaCO_3}$ values of the Mid-Holocene suggest the likely melting of all, or nearly all, of the annual snowmelt for that period. Positive excursions in the $\delta^{18}O_{CaCO_3}$ record at ~6,650 and ~4,880 cal. yBP are likely the result of periods of increased aridity and evaporative fractionation of oxygen isotopes of lake water. This theory is supported by coeval positive excursion in the $\delta^{13}C_{CaCO_3}$ record, indicative of increased aridity. Beginning ~3,000 cal. yBP, $\delta^{18}O_{CaCO_3}$ values increase steadily until 1,500 cal. yBP, indicative of increasing summer precipitation contribution to lake water. Values then decrease again until ~800 cal. yBP, again indicating an increase in snowmelt contribution-possibly due to warming temperatures coincident with Medieval Warming. Decadal variability persists from 800 cal. yBP to present with a mean $\delta^{18}O_{CaCO_3}$ value of -17.2‰ VPDB, consistent with modern marl values obtained in July 2006 of -17.2‰ (n =3), indicating that a similar water balance has persisted for the last ~850 years.

The Upper Hogarth Lake record provides evidence that marl lakes with short residence times and rapid, continuous sedimentation, can yield a high-resolution paleoenvironmental record. To better ascribe environmental conditions to stable isotope variability, it would be advantageous to compare and contrast these data with data generated from other studies in a given study area, (i.e. dendrochronology, palynology, and speleothem isotope analysis). It is critical that we fill-in continental gaps in paleoenvironmental records if we are to better understand regional climate variability and the cause of such paleoenvironmental change. An exponentially growing human population will place ever greater strain on Earth's water resources. We must understand how our freshwater lakes and headwaters have responded to climatic variability in the past in order to predict how human behavior will affect them in the future.

REFERENCES

Affolter, S., Fleitmann, D., and Leuenberger, M. 2014. New online method for water isotope analysis of speleothem fluid inclusions using laser absorption spectroscopy (WS-CRDS). Clim. Past, 10, 1291–1304. doi:10.5194/cp-10-1291-2014

Alberta Agriculture and Forestry and Environment and Parks, n.d. Alberta Weather Data [WWW Document]. URL https://agriculture.alberta.ca/acis/alberta-weather-data-viewer.jsp (accessed 9.28.18).

Alley, R.B., 2004. Abrupt Climate Change. Sci. Am. 291, 62–69.

Alley, R.B., Mayewski, P.A., Sowers, T., Stuiver, M., Taylor, K.C., Clark, P.A., 1997. Holocene climate variability: a prominent widespread event 8200 years ago. Geology 25, 483–486. doi:10.1130/0091-7613(1997)025<0483:HCIAPW>2.3.CO;2

Anderson, L., Abbott, M.B., Finney, B.P., Edwards, M.E., 2005. Palaeohydrology of the Southwest Yukon Territory, Canada, based on multiproxy analyses of lake sediment cores from a depth transect. Holocene 15, 1172–1183. doi:10.1191/0959683605hl889rp

Anderson, L., Berkelhammer, M., Barron, J.A., Steinman, B.A., Finney, B.P., Abbott, M.B., 2016. Lake oxygen isotopes as recorders of North American Rocky Mountain hydroclimate: Holocene patterns and variability at multi-decadal to millennial time scales. Glob. Planet. Change 137, 131–148. doi:10.1016/j.gloplacha.2015.12.021

Asmerom, Y., Polyak, V., Burns, S., Rassmssen, J., 2007. Solar forcing of Holocene climate: New insights from a speleothem record, southwestern United States. Geology 35, 1–4. doi:10.1130/G22865A.1

Barnett, T., Malone, R., Pennell, W., Stammer, D., Semtner, B., Washington, W., 2004. The Effects of Climate Change on Water Resources. Clim. Change 62, 1–11.

Beaudoin, A.B., King, R.H., 1994. Holocene palaeoenvironmental record preserved in a paraglacial alluvial fan, Sunwapta Pass, Jasper National Park, Alberta, Canada. Catena 22, 227–248. doi:10.1016/0341-8162(94)90004-3

Beierle, B., Smith, D.G., 1998. Severe drought in the early Holocene (10,000-6800 BP) interpreted from lake sediment cores, southwestern Alberta, Canada. Palaeogeogr. Palaeoclimatol. Palaeoecol. 140, 75–83. doi:10.1016/S0031-0182(98)00044-3

Beierle, B.D., 1997. Early Holocene Climate of Southwestern Alberta, Canada, Reconstructed From Lake Sediment Cores. University of Calgary. doi:10.16953/deusbed.74839

Beierle, B.D., Smith, D.G., Hills, L. V., Country, K., Beierle, B.D., Smith, D.G., Hills, L. V., 2003. Late Quaternary Glacial and Environmental History of the Burstall Pass Area, Kananaskis Country, Alberta, Canada. Arctic, Antarct. Alp. Res. 35, 391–398. doi:10.1657/1523-0430(2003)035[0391:LQGAEH]2.0.CO;2

Berger, A., Loutre, M.F., 1991. Insolation values for the climate of the last 10 million years. Quat. Sci. Rev. 10, 297–317.

Berger, A.L., 1979. Insolation Signatures of Quaternary Climatic Changes. Nuovo Cim. 2C, 63–87. doi:10.1007/BF02507714

Bianchi, G.G., McCave, I.N., 1999. Holocene periodicity in North Atlantic climate and deep-ocean fow south of Iceland. Arctic 35, 515–517. doi:10.1038/17362

Blindow, I., Hargeby, A., Andersson, G., 2002. Seasonal changes of mechanisms maintaining clear water in a shallow lake with abundant Chara vegetation. Aquat. Bot. 72, 315–334. doi:10.1016/S0304-3770(01)00208-X

Borzenkova, I., Zorita, E., Borisova, O., Kalnina, L., Kisieliene, D., Koff, T., Kuznetsov, D.,

Lemdahl, G., Sapelko, T., Stančikaitė, M., Subetto, D., 2015. Climate Change During the Holocene (Past 12,000 Years), in: Bolle, H.-J., al Vesuvio, S.S., Menenti, M., Rasool, S.I. (Eds.), Second Assessment of Climate Change for the Baltic Sea Basin. Springer International Publishing, Geesthacht, Germany, pp. 25–49. doi:10.1007/978-3-319-16006-1
Bow River Basin Council, 2010. State of the Watershed Summary, 2010. Calgary.
Bowling, D.R., Pataki, D.E., Randerson, J.T., 2008. Carbon Isotopes in Terrestrial Ecosystem Pools and CO_2 Fluxes. New Phytol. 178, 24–40. doi:10.2307/30147703
Clague, J.J., 2017. Deglaciation of the Cordillera of Western Canada at the end of the Pleistocene. Geogr. Res. Lett. 43, 449. doi:10.18172/cig.3232
Clague, J.J., Mathewes, R.W., Buhay, W.M., Edwards, T.R., 1992. Early Holocene climate at Castle Peak, south Coast Mountains, British Columbia, Canada. Palaeogeogr. Palaeoclimatol. Paleoecol. 95, 153–167.
Craig, H., 1957. Isotopic standards for carbon and oxygen and correction factors for mass-spectrometric analysis of carbon dioxide. Geochim. Cosmochim. Acta 12, 133–149. doi:10.1016/0016-7037(57)90024-8
Dansgaard, W., 1964. Stable isotopes in precipitation. Tellus 16, 436–468. doi:10.3402/tellusa.v16i4.8993
Davis, C.A., 1900. A Contribution to the Natural History of Marl. J. Geol. 8, 485–497. doi:10.1086/620841
De Boer, A.M., Nof, D., 2004. The exhaust valve of the North Atlantic. J. Clim. 17, 417–422. doi:10.1175/1520-0442(2004)017<0417:TEVOTN>2.0.CO;2
DeBeer, C.M., Wheater, H.S., Carey, S.K., Chun, K.P., 2016. Recent climatic, cryospheric, and hydrological changes over the interior of western Canada: A review and synthesis. Hydrol. Earth Syst. Sci. 20, 1573–1598. doi:10.5194/hess-20-1573-2016
Denton, G.H., Karlen, W., 1973. Holocene Climatic Variations-Their Pattern and Possible Cause 3, 155–205.
Diefendorf, A.F., Patterson, W.P., Holmden, C., Mullins, H.T., 2007. Carbon isotopes of marl and lake sediment organic matter reflect terrestrial landscape change during the late Glacial and early Holocene (16,800 to 5,540 cal yr B.P.): A multiproxy study of lacustrine sediments at Lough Inchiquin, western Ireland. J. Paleolimnol. 39, 101–115. doi:10.1007/s10933-007-9099-9
Downing, D.J., Pettapiece, W.W., 2006. Natural Regions and Subregions of Alberta. Gov. Alberta, 264 pp. doi:Pub. No. T/852
Drummond, C.N., Patterson, W.P., Walker, J.C.G., 1995. Climate forcing of carbon-oxygen isotopic covariance in temperate- region marl lakes. Geology 23, 1031–1034. doi:10.1130/0091-7613(1995)023<1031:CFOCOI>2.3.CO
Egan, J., Staff, R., Blackford, J., 2015. A high-precision age estimate of the Holocene Plinian eruption of Mount Mazama, Oregon, USA. Holocene 25, 1054–1067. doi:10.1177/0959683615576230
Epstein, S., Buchsbaum, R., Lowerstam, H.A., Urey, H.C., 1953. Revised Carbonate-Water Isotopic temperature scale 64.
Fisher, T.G., Smith, D.G., Andrews, J.T., 2002a. Preboreal oscillation caused by a glacial Lake Agassiz flood. Quat. Sci. Rev. 21, 873–878. doi:10.1016/S0277-3791(01)00148-2
Fisher, T.G., Smith, D.G., Andrews, J.T., 2002b. Preboreal oscillation caused by a glacial Lake Agassiz flood. Quat. Sci. Rev. 21, 873–878. doi:10.1016/S0277-3791(01)00148-2
García, A., 1994. Charophyta: their use in paleolimnology. J. Paleolimnol. 10, 43–52.

doi:10.1007/BF00683145
Garrels, R.M., Christ, C.L., 1965. Solutions, Minerals, and Equilibria, 1st ed. Harper & Row, New York.
Government-Of-Alberta, n.d. Alberta River Basins [WWW Document]. URL https://rivers.alberta.ca/ (accessed 10.25.18).
Heinrichs, M.L., Hebda, R.J., Walker, I.R., 2001. Holocene vegetation and natural disturbance in the Engelmann spruce - Subalpine fir biogeoclimatic zone at Mount Kobau, British Columbia. Can. J. For. Res. 31, 2183–2199. doi:10.1139/cjfr-31-12-2183
Hickman, M., Reasoner, M.A., 1998. Late quaternary diatom response to vegetation and climate change in a subalpine lake in Banff National Park, Alberta. J. Paleolimnol. 20, 253–265. doi:10.1023/A:1007978730349
Hood, J.L., Roy, J.W., Hayashi, M., 2006. Importance of groundwater in the water balance of an alpine headwater lake. Geophys. Res. Lett. 33, 1–5. doi:10.1029/2006GL026611
Houghton, J.T., Ding, Y., Griggs, D.J., Noguer, M., van der Linden, P.J., Dai, X., Maskell, K., Johnson, C.A., 2001. Climate Change 2001: The Scientific Basis. Clim. Chang. 2001 Sci. Basis 881. doi:10.1256/004316502320517344
Hren, M.T., Sheldon, N.D., 2012. Temporal variations in lake water temperature: Paleoenvironmental implications of lake carbonate δ18O and temperature records. Earth Planet. Sci. Lett. 337–338, 77–84. doi:10.1016/j.epsl.2012.05.019
Hu, A., Meehl, G. a., Otto-Bliesner, B.L., Waelbroeck, C., Han, W., Loutre, M.-F., Lambeck, K., Mitrovica, J.X., Rosenbloom, N.A., 2010. Influence of Bering Strait flow and North Atlantic circulation on glacial sea-level changes. Nat. Geosci. 3, 118–121. doi:10.1038/ngeo729
Hu, A., Meehl, G.A., Han, W., Timmermann, A., Otto-Bliesner, B., Liu, Z., Washington, W.M., Large, W., Abe-Ouchi, A., Kimoto, M., Lambeck, K., Wu, B., 2012. Role of the Bering Strait on the hysteresis of the ocean conveyor belt circulation and glacial climate stability. Proc. Natl. Acad. Sci. 109, 6417–6422. doi:10.1073/pnas.1116014109
International Atomic Energy Agency, 2013. Isotope Hydrology Publications [WWW Document]. Environ. Isot. Hydrol. Cycle. URL http://www-naweb.iaea.org/napc/ih/IHS_resources_publication_hydroCycle_en.html
Kamae, Y., Mei, W., Xie, S.P., Naoi, M., Ueda, H., 2017. Atmospheric rivers over the Northwestern Pacific: Climatology and interannual variability. J. Clim. 30, 5605–5619. doi:10.1175/JCLI-D-16-0875.1
Kaufman, D.S., Ager, T.A., Anderson, N.J., Anderson, P.M., Andrews, J.T., Bartlein, P.J., Brubaker, L.B., Coats, L.L., Cwynar, L.C., Duvall, M.L., Dyke, A.S., Edwards, M.E., Eisner, W.R., Gajewski, K., Geirsdóttir, A., Hu, F.S., Jennings, A.E., Kaplan, M.R., Kerwin, M.W., Lozhkin, A. V., MacDonald, G.M., Miller, G.H., Mock, C.J., Oswald, W.W., Otto-Bliesner, B.L., Porinchu, D.F., Rühland, K., Smol, J.P., Steig, E.J., Wolfe, B.B., 2004. Holocene thermal maximum in the western Arctic (0-180°W). Quat. Sci. Rev. 23, 529–560. doi:10.1016/j.quascirev.2003.09.007
Kendall, C., McDonnell, J.J., 1998. Isotope Tracers in Catchment Hydrology, 1st ed. Elsevier B.V.
Kim, S.-T., O'Neil, J.R., 1997. Equilibrium and nonequilibrium oxygen isotope effects in synthetic carbonates. Geochim. Cosmochim. Acta 61, 3461–3475. doi:10.1016/S0016-7037(97)00169-5
Kirby, M., Patterson, W., Mullins, H., Burnett, A., 2002. Post-Younger Dryas climate interval

linked to circumpolar vortex variability: Isotopic evidence from Fayetteville Green Lake, New York. Clim. Dyn. 19, 321–330. doi:10.1007/s00382-002-0227-y
Kreutz, K.J., Mayewski, P.A., Meeker, L.D., Twickler, M.S., Whitlow, S.I., Pittalwala, I.I., 1997. Bipolar Changes in Atmospheric Circulation During the Little Ice Age. Science (80-.). 277, 1294–1296.
Lapp, S., Byrne, J., Kienzle, S., Townshend, I., 2002. Linking Global Circulation Model synoptics and precipitation for western North America. Int. J. Climatol. 22, 1807–1817. doi:10.1002/joc.851
Leng, M.J., Marshall, J.D., 2004. Palaeoclimate interpretation of stable isotope data from lake sediment archives. Quat. Sci. Rev. 23, 811–831. doi:10.1016/j.quascirev.2003.06.012
Leonard, E.M., Reasoner, M.A., 1999. A continuous holocene glacial record inferred from proglacial lake sediments in Banff National Park, Alberta, Canada. Quat. Res. 51, 1–13. doi:10.1006/qres.1998.2009
Lischeid, G., Kalettka, T., Holländer, M., Steidl, J., Merz, C., Dannowski, R., Hohenbrink, T., Lehr, C., Onandia, G., Reverey, F., Pätzig, M., 2018. Natural ponds in an agricultural landscape: External drivers, internal processes, and the role of the terrestrial-aquatic interface. Limnologica 68, 5–16. doi:10.1016/j.limno.2017.01.003
Luckman, B.H., Kearney, M.S., 1986. Reconstruction of Holocene Changes in Alpine Vegetation and Climate in the Maligne Range, Jasper National Park, Alberta. Quat. Res. 26, 244–261.
Macdonald, G.M., 1989. Postglacial Palaeoecology of the Subalpine Forest - Grassland Ecotone of Southwestern Alberta: New Insights on Vegetation and Climate Change in The Canadian Rocky Mountains and Adjacent Foothills. Elsevier Sci. Publ. B.V 73, 155–173.
Macdonald, G.M., 1987. Postglacial Development of the Subalpine-Boreal Transition Forest of Western Canada. J. Ecol. 75, 303–320.
Macdonald, G.M., 1981. Late Quaternary paleoenvironments of the Morley Flats and Kananaskis Valley of southwestern Alberta. Can. J. Earth Sci. 19, 23–35.
Mann, M.E., Zhang, Z., Rutherford, S., Bradley, R.S., Hughes, M.K., Shindell, D., Ammann, C., Faluvegi, G., Ni, F., 2009. Medieval Climate Anomaly. Science (80-.). 326, 1256–1260. doi:10.1126/science.1166349
Mathewes, R.W., Heusser, L.E., 1980. A 12 000 year palynological record of temperature and precipitation trends in southwestern British Columbia. Can. J. Bot. 59, 707–710.
Mcconnaughey, T., 1991. Calcification in Chara coralina: CO2 hydroxylation generates protons for bicarbonate assimilation. Limnol. Oceanogr. 36, 619–628.
Mcconnaughey, T.A., Falk, R.H., Mcconnaugheyl, T.E.D.A., Falk, R.H., 1991. Calcium-Proton Exchange During Algal Calcification. Biol. Bull. 180, 185–195.
McConnaughey, T.A., Labaugh, J.W., Rosenberry, D.O., Striegl, R.G., Labaugh, J.W., 1994. Carbon budget for a groundwater-fed lake: Calcification supports summer photosynthesis. Limnol. Oceanogr. 39, 1319–1332. doi:10.4319/lo.1994.39.6.1319
Mcconnaughey, T.A., Striegl, R.G., Labaugh, J.W., 1994. Carbon budget for a groundwater-fed lake : Calcification supports summer photosynthesis 39, 1319–1332.
McCrea, J.M., 1950. On the isotope chemistry of carbonates and a palaeotemperature scale. Jour. Chem. Phys. 18, 849–857.
Milrad, S.M., Gyakum, J.R., Atallah, E.H., 2015. A Meteorological Analysis of the 2013 Alberta Flood: Antecedent Large-Scale Flow Pattern and Synoptic–Dynamic Characteristics. Mon. Weather Rev. 143, 2817–2841. doi:10.1175/MWR-D-14-00236.1

Moran, T., Marshall, S., Evans, E., Sinclair, K., 2007. Altitudinal Gradients of Stable Isotopes in Lee-Slope Precipitation in the Canadian Rocky Mountains. Arctic, Antarct. Alp. Res. Alp. Res. 39, 455–467. doi:10.1657/1523-0430(06-022)

Mullins, H.T., Patterson, W.P., Teece, M.A., Burnett, A.W., 2011. Holocene climate and environmental change in central New York (USA). J. Paleolimnol. 45, 243–256. doi:10.1007/s10933-011-9495-z

Murphy, D.H., Wilkinson, B.H., 1980. Carbonate deposition and facies distribution in a central Michigan marl lake. Sedimentology 27, 123–135. doi:10.1111/j.1365-3091.1980.tb01164.x

National Oceanic and Atmospheric Administration (NOAA), (NRC), U.S.N.R.C., 1985. Climate of Idaho [WWW Document].

Patterson, W.P., 2017. Environmental Stable Isotope Chemistry, 1st ed. Kendal Hunt Publishing.

Pełechaty, M., Pukacz, A., Apolinarska, K., Pełechata, A., Siepak, M., 2013. The significance of Chara vegetation in the precipitation of lacustrine calcium carbonate. Sedimentology 60, 1017–1035. doi:10.1111/sed.12020

Pendleton, S.L., Miller, G.H., Anderson, R.A., Crump, S.E., Zhong, Y., Jahn, A., Geirsdottir, Á., 2017. Episodic Neoglacial expansion and rapid 20th century retreat of a small ice cap on Baffin Island, Arctic Canada, and modeled temperature change. Clim. Past 13, 1527–1537. doi:10.5194/cp-13-1527-2017

Peng, H., Mayer, B., Harris, S., Krouse, H.R., 2004. A 10-year record of stable isotope ratios of hydrogen and oxygen in precipitation at Calgary, Alberta, Canada. Tellus, Ser. B Chem. Phys. Meteorol. 56, 147–159. doi:10.1111/j.1600-0889.2004.00094.x

Platt, N.H., Wright, V.P., 2009. Lacustrine Carbonates: Facies Models, Facies Distributions and Hydrocarbon Aspects. Lacustrine Facies Anal., Wiley Online Books. doi:doi:10.1002/9781444303919.ch3

Pomeroy, J.W., Stewart, R.E., Whitfield, P.H., 2016. The 2013 flood event in the South Saskatchewan and Elk River basins: Causes, assessment and damages. Can. Water Resour. J. 41, 105–117. doi:10.1080/07011784.2015.1089190

Reasoner, M.A., Healy, R.E., 1986. Identification and significance of tephras encaudered in a core from Mary Lake, Yoho National Park, British Columbia. Candian J. Earth Sci. 23, 1991–1999. doi:10.1139/e86-184

Reasoner, M.A., Hickman, M., 1989. Late Quaternary environmental change in the Lake O'Hara region, Yoho National Park, British Columbia. Palaeogeogr. Palaeoclimatol. Palaeoecol. 72, 291–316. doi:10.1016/0031-0182(89)90149-1

Reasoner, M.A., Huber, U.M., 1999. Postglacial palaeoenvironments of the upper Bow Valley, Banff National Park, Alberta, Canada. Quat. Sci. Rev. 18, 475–492. doi:10.1016/S0277-3791(98)00034-1

Reasoner, M.A., Jodry, M.A., 2000. Rapid response of alpine timberline vegetation to the Younger Dryas climate oscillation in the Colorado Rocky Mountains, USA. Geology 28, 51–54. doi:10.1130/0091-7613(2000)28<51:RROATV>2.0.CO;2

Reimer, P.J., Bard, E., Bayliss, A., Beck, J.W., Blackwell, P.G., Ramsey, C.B., Buck, C.E., Cheng, H., Edwards, R.L., Friedrich, M., Grootes, P.M., Guilderson, T.P., Haflidason, H., Hajdas, I., Hatté, C., Heaton, T.J., Hoffmann, D.L., Hogg, A.G., Hughen, K.A., Kaiser, K.F., Kromer, B., Manning, S.W., Niu, M., Reimer, R.W., Richards, D.A., Scott, E.M., Southon, J.R., Staff, R.A., Turney, C.S.M., van der Plicht, J., 2013. IntCal13 and Marine13 Radiocarbon Age Calibration Curves 0–50,000 Years cal BP. Radiocarbon 55, 1869–1887. doi:DOI: 10.2458/azu_js_rc.55.16947

Renssen, H., Seppä, H., Crosta, X., Goosse, H., Roche, D.M., 2012. Global characterization of the Holocene Thermal Maximum. Quat. Sci. Rev. 48, 7–19. doi:10.1016/j.quascirev.2012.05.022

Renssen, H., Seppä, H., Heiri, O., Roche, D.M., Goosse, H., Fichefet, T., 2009. The spatial and temporal complexity of the holocene thermal maximum. Nat. Geosci. 2, 411–414. doi:10.1038/ngeo513

Reyes, A. V., Wiles, G.C., Smith, D.J., Barclay, D.J., Allen, S., Jackson, S., Larocque, S., Laxton, S., Lewis, D., Calkin, P.E., Clague, J.J., 2006. Expansion of alpine glaciers in Pacific North America in the first millennium A.D. Geology 34, 57–60. doi:10.1130/G21902.1

Rozanski, K., Araguãs-Araguãs, L., Gonfiantini, R., 1992. Relation between long-term trends of oxygen-18 isotope composition of precipitation and climate. Science (80-.). 258, 981–985. doi:10.1126/science.258.5084.981

Scott, C., 2013. Alberta floods. Why is there so much rain? [WWW Document]. Insid. Insights Artic. - Weather Netw. URL https://www.theweathernetwork.com/insider-insights/articles/alberta-floods-why-is-there-so-much-rain/8124/ (accessed 8.31.18).

Shapley, M.D., Ito, E., Donovan, J.J., 2009. Lateglacial and Holocene hydroclimate inferred from a groundwater flow-through lake, Northern Rocky Mountains, USA. The Holocene 19, 523–535. doi:10.1177/0959683609104029

Shuman, B.N., Marsicek, J., 2016. The structure of Holocene climate change in mid-latitude North America. Quat. Sci. Rev. 141, 38–51. doi:10.1016/j.quascirev.2016.03.009

Smith, D.G., 1998. Vibracoring: A new method for coting deep lakes. Palaeogeogr. Palaeoclimatol. Palaeoecol. 140, 433–440. doi:10.1016/S0031-0182(98)00031-5

Steinman, B.A., Abbott, M.B., 2013. Isotopic and hydrologic responses of small, closed lakes to climate variability: Hydroclimate reconstructions from lake sediment oxygen isotope records and mass balance models. Geochim. Cosmochim. Acta 105, 342–359. doi:10.1016/j.gca.2012.11.027

Stuiver, M., 1970. Oxygen and carbon isotope ratios of fresh-water carbonates as climatic indicators. J. Geophys. Res. 75, 5247–5257. doi:10.1029/JC075i027p05247

Talbot, M.R., 1990. A review of the palaeohydrological interpretation of carbon and oxygen isotopic ratios in primary lacustrine carbonates. Chem. Geol. Isot. Geosci. Sect. 80, 261–279. doi:10.1016/0168-9622(90)90009-2

Teller, J.T., 2003. Controls, history, outbursts, and impact of large late-Quaternary proglacial lakes in North America. Dev. Quat. Sci. 1, 45–61. doi:10.1016/S1571-0866(03)01003-0

Teller, J.T., Leverington, D.W., Mann, J.D., 2002. Freshwater outbursts to the oceans from glacial Lake Agassiz and their role in climate change during the last deglaciation. Quat. Sci. Rev. 21, 879–887. doi:10.1016/S0277-3791(01)00145-7

Teranes, J.L., McKenzie, J.A., Bernasconi, S.M., Lotter, A.F., Sturm, M., 1999. A study of oxygen isotopic fractionation during bio-induced calcite precipitation in eutrophic Baldeggersee, Switzerland. Geochim. Cosmochim. Acta 63, 1981–1989. doi:10.1016/S0016-7037(99)00049-6

Thériault, J.M., Hung, I., Vaquer, P., Stewart, R.E., Pomeroy, J.W., 2018. Precipitation characteristics and associated weather conditions on the eastern slopes of the Canadian Rockies during March–April 2015. Hydrol. Earth Syst. Sci. 22, 4491–4512.

Toop, D.C., de la Cruz, N.N., 2002. Hydrogeology of the Canmore Corridor and Northwestern Kananaskis Country, Alberta. p. 84.

Van Der Ent, R.J., Savenije, H.H.G., 2013. Oceanic sources of continental precipitation and the correlation with sea surface temperature. Water Resour. Res. 49, 3993–4004. doi:10.1002/wrcr.20296

Vance, R.E., 1986. Aspects of the postglacial climate of Alberta: Calibration of the pollen record. Geogr. Phys. Quat. 40, 153–160.

Vartanyan, S.L., 1997. The last Beringian survivors: Interdisciplinary paleogeographical studies on Wrangel Island, east Siberia. Florissant, CO.

Viau, A.E., Gajewski, K., Sawada, M.C., Fines, P., 2006. Millennial-scale temperature variations in North America during the Holocene. J. Geophys. Res. Atmos. 111, 1–12. doi:10.1029/2005JD006031

Vincent, W.F., 2009. Effects of Climate Change on Lakes, in: Likens, G.E.B.T.-E. of I.W. (Ed.), . Academic Press, Oxford, pp. 55–60. doi:https://doi.org/10.1016/B978-012370626-3.00233-7

Wanner, H., Solomina, O., Grosjean, M., Ritz, S.P., Jetel, M., 2011. Structure and origin of Holocene cold events. Quat. Sci. Rev. 30, 3109–3123. doi:10.1016/j.quascirev.2011.07.010

Watson, E., Luckman, B.H., 2006. Long Hydroclimate Records from Tree-Rings in Western Canada: Potential, Problems and Prospects. Can. Water Resour. J. 31, 205–228. doi:10.4296/cwrj3104205

Wehr, J.D., Sheath, R.G., 2015. Habitats of Freshwater Algae, Freshwater Algae of North America: Ecology and Classification. doi:10.1016/B978-0-12-385876-4.00002-5

Wynn, J.G., 2007. Carbon isotope fractionation during decomposition of organic matter in soils and paleosols: Implications for paleoecological interpretations of paleosols. Palaeogeogr. Palaeoclimatol. Palaeoecol. 251, 437–448. doi:10.1016/j.palaeo.2007.04.009

Zdanowicz, C.M., Zielinski, G.A., Germani, M.S., 1999. Mount Mazama eruption: Calendrical age verified and atmospheric impact assessed. Geology 27, 621–624. doi:10.1130/0091-7613(1999)027<0621:MMECAV>2.3.CO

APPENDIX: $\delta^{18}O_{CaCO_3}$ and $\delta^{13}C_{CaCO_3}$ values of Upper Hogarth Lake Marl

Depth (mm)	Age (cal. yBP)	$\delta^{18}O_{CaCO3}$	$\delta^{13}C_{CaCO3}$
1	-55	-16.8	-2.0
2	-51	-16.7	-2.0
3	-46	-17.1	-2.6
4	-42	-17.0	-2.9
5	-37	-17.0	-2.3
6	-33	-17.1	-2.0
7	-28	-16.8	-2.2
8	-24	-16.6	-0.9
9	-19	-17.6	-2.9
10	-15	-17.5	-3.1
11	-10	-17.1	-3.1
12	-6	-17.1	-2.9
13	-1	-16.9	-2.8
14	3	-17.4	-2.0
15	8	-16.6	-0.9
16	12	-16.4	-0.3
17	17	-17.4	-2.2
18	21	-17.2	-1.5
19	26	-17.3	-1.7
20	30	-17.0	-1.4
21	35	-17.5	-1.9
22	39	-17.6	-1.9
23	44	-17.8	-1.5
24	48	-17.5	-0.9
25	53	-17.6	-1.0
26	57	-17.2	-1.3
27	62	-17.1	-1.2
28	66	-17.2	-1.9
29	71	-17.1	-1.8
30	75	-17.0	-1.5
31	80	-16.9	-1.4
32	84	-16.9	-1.3
33	89	-17.3	-1.2
34	93	-17.5	-1.4
35	98	-17.3	-0.9
36	102	-17.4	-0.7

37	107	-16.6	-0.1
38	111	-16.8	-0.9
39	116	-17.0	-1.2
40	120	-16.8	-0.8
41	125	-16.9	-0.9
42	129	-16.7	-0.8
43	134	-17.1	-0.9
44	138	-17.2	-1.2
45	143	-17.4	-1.4
46	147	-17.4	-1.2
47	152	-17.8	-1.5
48	156	-17.3	-1.4
49	161	-17.1	-0.9
50	165	-16.9	-0.6
51	170	-17.1	-1.1
52	174	-16.9	-1.1
53	179	-16.6	-0.5
54	183	-16.8	-1.1
55	188	-16.8	-1.2
56	192	-16.7	-1.5
58	201	-17.0	-1.7
60	210	-16.7	-0.9
62	219	-17.2	-1.7
64	228	-17.2	-2.0
66	237	-16.9	-1.2
68	246	-17.5	-1.5
70	255	-17.3	-1.3
72	264	-17.3	-1.3
74	273	-17.2	-1.9
76	282	-17.1	-1.3
78	291	-17.2	-1.5
80	300	-17.1	-1.4
82	309	-17.4	-1.7
84	318	-17.3	-1.8
86	327	-17.4	-1.9
88	336	-17.6	-1.8
90	345	-17.6	-1.7
92	354	-17.6	-1.9
94	363	-17.4	-1.8

96	372	-17.4	-1.5
98	381	-17.7	-1.7
100	390	-17.4	-1.4
102	399	-17.4	-1.4
104	408	-17.3	-1.1
106	417	-17.6	-1.2
108	426	-17.2	-0.8
110	435	-17.3	-1.2
112	444	-17.2	-1.2
114	453	-17.2	-1.5
116	462	-17.2	-1.2
118	471	-17.0	-1.4
120	480	-17.1	-1.6
122	489	-17.0	-1.2
124	498	-17.2	-2.0
126	507	-17.3	-1.6
128	516	-17.2	-1.9
130	525	-17.2	-1.9
132	534	-17.3	-3.0
134	543	-17.4	-2.0
136	552	-17.4	-1.7
138	561	-17.3	-1.6
140	570	-17.4	-1.8
142	579	-17.3	-2.3
144	588	-17.4	-1.8
146	597	-17.5	-1.2
148	606	-17.5	-1.1
150	615	-17.7	-1.2
152	624	-17.3	-1.6
154	633	-17.2	-1.3
156	642	-17.3	-1.3
158	651	-17.2	-1.1
160	660	-17.3	-1.4
162	669	-17.3	-1.5
164	678	-17.7	-1.6
166	687	-17.7	-1.9
168	696	-17.6	-2.3
170	705	-17.6	-2.2
172	714	-17.7	-2.1

174	723	-18.0	-2.3
176	732	-17.9	-3.0
178	741	-18.0	-3.0
180	750	-17.7	-2.7
182	759	-17.3	-1.2
184	768	-17.3	-2.0
186	777	-17.2	-1.4
188	786	-17.4	-1.8
190	795	-17.4	-1.6
192	804	-17.3	-2.0
194	813	-17.4	-1.0
196	822	-17.4	-0.6
198	831	-17.7	-0.9
200	840		
202	849	-17.8	-2.1
204	858	-17.5	-1.4
206	867	-17.3	0.0
208	876	-17.7	-2.3
210	885	-17.3	-0.4
212	894	-17.2	-0.7
214	903	-16.7	-0.1
216	912	-16.6	-0.7
218	921	-16.8	-1.0
220	930	-17.1	-1.2
222	939	-17.1	-1.3
224	948	-17.5	-1.5
226	957	-17.5	-1.7
228	966	-17.4	-3.4
230	975	-17.4	-2.2
232	984	-17.4	-1.8
234	993	-17.3	-1.2
236	1002	-17.4	-1.5
238	1011	-17.2	-1.4
240	1021	-17.3	-1.1
242	1030	-17.4	-1.8
243	1034	-17.3	-2.6
244	1039	-17.7	-2.7
246	1048	-18.0	-1.7
247	1052	-17.8	-1.6

248	1057	-17.5	-2.5
249	1061	-18.0	-3.4
250	1066	-18.1	-3.1
251	1070		
252	1075	-18.1	-3.3
254	1084	-17.7	-3.3
255	1088	-17.9	-3.6
256	1093	-17.7	-3.8
257	1097	-17.5	-3.0
258	1102	-17.6	-3.4
259	1106	-17.5	-3.3
260	1111	-17.5	-3.3
261	1115	-17.1	-3.0
262	1120	-17.0	-1.8
263	1124	-17.4	-2.1
264	1129	-17.3	-1.8
266	1138	-17.4	-1.0
268	1147	-17.4	-1.3
270	1156	-17.5	-1.3
272	1165	-17.3	-1.1
274	1174	-16.7	-0.4
276	1183	-17.3	-0.6
278	1192	-17.5	-1.3
280	1201	-17.4	-1.0
282	1210	-17.1	-0.5
284	1219	-16.9	-0.7
286	1228	-16.5	0.4
291	1248	-17.2	-1.1
295	1268	-17.1	-0.3
299	1288	-17.0	-0.8
304	1308	-17.8	-1.5
308	1328	-17.4	-0.4
313	1348	-17.3	-0.5
317	1368	-16.9	-0.2
322	1388	-17.4	-0.6
326	1408	-17.1	-1.2
331	1428	-17.1	-1.5
335	1448	-16.8	-1.2
339	1468	-16.7	-0.9

344	1488	-16.8	-0.8
348	1508	-17.2	-0.9
353	1528	-16.9	0.2
357	1548	-16.6	-1.2
362	1568	-16.6	-0.9
366	1588	-16.6	-0.5
370	1608	-16.9	-1.1
375	1628	-16.9	-1.2
379	1647	-16.9	-1.3
384	1667	-16.8	-1.3
388	1687	-17.2	-1.2
393	1707	-17.4	-1.2
397	1727	-17.4	-1.9
402	1748	-17.2	-1.2
406	1769	-17.4	-0.9
411	1789	-17.1	-1.7
415	1810	-17.0	-1.3
420	1831	-17.0	-1.0
425	1852	-17.0	-1.5
429	1872	-16.7	-2.2
434	1893	-17.2	-1.6
438	1914	-17.4	-1.6
443	1934	-17.3	-1.7
448	1955	-17.7	-1.7
452	1976	-17.8	-0.8
457	1997	-16.9	-1.4
461	2017	-16.9	-1.6
466	2038	-17.0	-1.7
471	2059	-16.9	-1.4
475	2079	-17.0	-1.4
480	2100	-17.1	-1.2
484	2121	-17.7	-1.2
489	2142	-17.2	-1.0
494	2162	-17.3	-0.8
498	2183	-17.6	-0.6
503	2204	-17.4	-0.8
507	2224	-17.2	-0.6
512	2245	-17.5	-0.5
517	2266	-17.5	-0.9

521	2286	-16.9	-1.7
526	2307	-17.3	-1.9
530	2328	-17.7	-1.8
535	2349	-17.3	-1.1
540	2369	-17.1	-0.9
544	2389	-17.1	-0.8
549	2409	-17.6	-1.0
553	2430	-17.5	-0.6
558	2450	-17.4	0.3
562	2470	-17.5	-1.0
567	2490	-17.5	-0.6
571	2511	-17.6	-0.2
576	2531	-16.8	0.6
580	2551	-17.0	0.1
585	2571	-17.4	-0.8
589	2592	-17.3	-0.4
594	2612	-17.6	-0.2
598	2632	-17.6	-0.8
603	2653	-17.6	-1.2
607	2673	-17.6	-0.3
612	2693	-17.8	-0.7
616	2713	-17.7	0.0
621	2734	-17.7	0.1
625	2754	-17.7	-0.1
630	2774	-17.1	-0.3
634	2794	-17.6	-0.3
639	2815	-18.0	-0.5
643	2835	-17.3	-1.0
648	2855	-17.5	1.0
652	2875	-18.1	-0.7
657	2896	-18.0	0.5
661	2916	-18.0	0.2
666	2936	-17.6	-0.2
670	2956	-18.4	-0.3
675	2977	-17.7	0.3
679	2997	-17.7	0.1
684	3017	-17.7	-0.8
688	3037	-18.1	-0.7
693	3058	-18.0	-1.1

697	3078	-17.9	-0.8
702	3098	-18.1	0.0
706	3118	-18.0	-1.2
711	3139	-18.1	-0.7
715	3159	-17.9	-0.7
720	3179	-18.0	-0.5
724	3200	-17.6	-0.8
729	3220	-18.4	-0.4
733	3240	-18.0	-1.2
738	3260	-17.6	-1.2
742	3281	-18.0	-1.1
747	3301	-17.8	-1.2
751	3321	-17.7	-1.3
756	3341	-17.8	-0.8
760	3362	-18.0	-1.1
765	3382	-18.1	-0.6
769	3402	-18.2	-0.8
774	3422	-18.3	-0.3
778	3443	-18.2	-1.0
783	3463	-18.3	0.0
787	3483	-17.7	-1.1
792	3503	-17.6	-0.2
796	3524	-17.7	-0.1
801	3544	-17.7	-0.2
805	3564	-17.2	-0.9
810	3585	-18.1	-0.4
814	3605	-18.2	-1.1
819	3626	-18.4	-0.4
823	3646	-18.1	-0.1
828	3667	-17.9	-0.8
832	3688	-18.5	-0.2
837	3708	-18.4	0.2
842	3729	-17.8	-0.6
846	3749	-17.8	-0.9
851	3770	-18.2	0.0
855	3790	-17.5	-0.1
860	3811	-17.5	0.1
864	3831	-18.6	-0.7
869	3852	-17.4	0.0

874	3873	-17.9	-0.4
878	3893	-17.9	-0.3
883	3914	-17.9	-1.4
887	3934	-17.9	0.2
892	3955	-17.9	-0.3
896	3975	-17.8	-0.3
901	3996	-18.1	-0.3
905	4017	-18.3	0.1
910	4037	-18.3	0.2
915	4058	-18.4	-0.4
919	4078	-18.3	0.4
924	4099	-18.1	-0.5
928	4119	-18.1	-0.7
933	4140	-17.7	-0.3
937	4160	-18.2	-0.6
942	4181	-17.5	0.4
947	4202	-18.3	-0.2
951	4222	-17.7	-0.2
956	4243	-17.9	-0.2
960	4264	-18.1	-1.7
965	4285	-17.3	-0.5
970	4305	-17.8	-1.0
974	4326	-18.1	-0.9
979	4347	-17.8	-0.3
983	4367	-17.2	0.2
988	4388	-17.4	0.2
993	4409	-17.5	-0.3
997	4429	-17.6	-0.4
1002	4450	-17.6	-0.3
1006	4471	-17.5	-0.7
1011	4492	-17.3	0.4
1016	4512	-17.4	0.2
1020	4533	-17.2	0.3
1025	4554	-17.4	-0.3
1029	4574	-18.1	-0.3
1034	4595	-17.7	0.5
1039	4616	-18.1	0.1
1043	4637	-18.2	-0.1
1048	4657	-18.1	-1.3

1052	4678	-17.5	0.7
1057	4699	-17.7	0.7
1062	4719	-18.0	0.2
1066	4740	-18.0	0.5
1071	4761	-18.2	0.1
1075	4782	-17.7	0.4
1080	4802	-17.9	1.1
1085	4823	-17.7	0.6
1089	4843	-16.8	1.0
1094	4864	-16.8	1.3
1098	4884	-16.2	0.5
1103	4905	-17.2	-0.2
1107	4925	-17.6	-0.2
1112	4946	-17.5	-0.3
1116	4966	-17.6	-0.2
1121	4987	-17.8	0.1
1125	5007	-18.1	-0.3
1130	5028	-18.0	0.4
1135	5048	-18.2	0.1
1139	5068	-18.0	0.2
1144	5089	-18.0	-0.2
1148	5109	-18.3	-0.8
1153	5130	-18.0	-0.2
1157	5150	-17.8	0.4
1162	5171	-18.0	0.3
1166	5191	-18.2	-0.7
1171	5212	-17.5	0.9
1176	5232	-17.8	0.4
1180	5253	-17.7	0.4
1185	5273	-17.9	0.0
1189	5294	-18.6	0.0
1194	5314	-17.9	-0.1
1198	5335	-18.3	-0.1
1203	5355	-18.4	0.9
1207	5376	-18.5	0.3
1212	5396	-18.2	0.6
1216	5417	-17.6	1.2
1221	5437	-17.6	1.1
1226	5458	-18.2	0.1

1230	5478	-17.9	0.6
1235	5499	-18.1	0.9
1239	5520	-17.9	0.8
1244	5541	-18.1	-0.6
1249	5561	-18.6	-0.1
1253	5582	-18.0	0.3
1258	5603	-18.0	0.5
1262	5623	-18.8	1.3
1267	5644	-18.5	0.5
1272	5665	-18.2	0.1
1276	5686	-17.2	1.1
1281	5706	-17.3	1.6
1285	5727	-17.6	1.1
1290	5748	-17.4	1.1
1295	5768	-17.8	0.5
1299	5789	-18.1	0.2
1304	5810	-17.6	0.3
1308	5831	-18.3	-0.9
1313	5851	-18.4	-1.3
1318	5872	-17.8	0.6
1322	5893	-18.0	1.0
1327	5913	-18.3	-0.2
1331	5934	-18.2	0.4
1336	5955	-18.1	-1.8
1341	5976	-17.8	0.9
1345	5996	-17.9	0.8
1350	6017	-18.4	0.7
1354	6038	-18.4	0.2
1359	6058	-18.4	0.3
1364	6079	-18.6	0.5
1368	6099	-17.6	0.2
1373	6120	-18.0	0.2
1377	6141	-18.4	0.1
1382	6161	-17.9	0.5
1386	6182	-18.2	0.2
1391	6202	-18.8	-0.2
1396	6223	-18.3	0.1
1400	6243	-17.8	-0.1
1405	6264	-18.1	0.2

1409	6285	-18.5	0.3
1414	6305	-18.0	0.8
1418	6326	-18.4	0.3
1423	6346	-17.7	0.9
1428	6367	-18.1	0.8
1432	6387	-18.3	0.4
1437	6408	-17.9	0.5
1441	6428	-17.9	0.4
1446	6449	-18.2	0.3
1450	6470	-18.8	-0.1
1455	6490	-18.5	0.0
1459	6511	-18.1	0.4
1464	6531	-17.9	0.4
1469	6552	-18.1	0.4
1473	6572	-18.2	0.7
1478	6593	-18.0	0.5
1482	6613	-18.2	0.4
1487	6634	-17.2	1.2
1491	6655	-16.8	1.0
1496	6675	-17.8	1.1
1500	6695	-17.3	0.5
1505	6715	-17.2	0.8
1509	6736	-17.2	0.7
1514	6756	-18.0	-0.2
1518	6776	-18.2	-0.2
1523	6796	-18.1	0.4
1527	6816	-18.3	0.6
1532	6836	-18.2	0.6
1536	6857	-18.3	0.3
1541	6877	-18.6	0.9
1545	6897	-18.0	-0.1
1550	6917	-18.1	0.8
1554	6937	-18.1	0.2
1559	6957	-18.3	0.4
1563	6978	-18.4	0.0
1568	6998	-18.2	-0.4
1572	7018	-18.4	0.3
1577	7038	-18.2	-0.6
1581	7058	-18.3	0.3

1586	7078	-18.0	0.6
1590	7099	-17.5	1.0
1595	7119	-18.4	-0.7
1599	7139	-17.9	0.6
1604	7159	-17.8	0.4
1610	7188	-18.1	0.2
1617	7220	-18.7	-0.3
1621	7238	-18.3	-0.5
1626	7260	-18.2	-0.5
1630	7280	-18.0	-0.2
1635	7300	-17.3	0.3
1639	7320	-17.7	-0.3
1644	7341	-17.7	-1.0
1648	7361	-18.1	-0.8
1653	7381	-17.6	-0.9
1657	7401	-17.6	-1.7
1662	7421	-18.3	-1.5
1666	7441	-17.4	-0.9
1668	7450	-18.1	-0.5
1673	7472	-18.2	-0.3
1679	7499		
1681	7508		
1685	7526		
1690	7549		
1694	7567		
1699	7589		
1704	7610	-18.0	-0.6
1708	7630	-18.1	-0.1
1713	7651	-18.0	-0.2
1717	7671	-17.8	-0.3
1722	7691	-17.9	-0.2
1726	7711	-17.6	0.2
1731	7731	-17.7	-0.2
1735	7751	-17.9	-0.1
1739	7771	-17.7	0.2
1744	7791	-17.2	-0.4
1748	7811	-17.5	0.5
1753	7832	-16.8	0.9
1757	7852	-16.5	0.4

1762	7872	-17.2	0.2
1766	7892	-18.0	0.4
1771	7912	-17.9	0.0
1775	7932	-17.8	0.0
1780	7952	-17.6	0.5
1784	7972	-17.9	-0.9
1789	7992	-17.8	-1.0
1793	8013	-17.8	0.1
1798	8033	-17.6	0.7
1802	8053	-17.5	0.6
1807	8073	-17.6	0.0
1811	8094	-17.2	0.2
1816	8114	-16.8	0.2
1820	8134	-17.4	0.0
1825	8155	-16.7	-0.5
1829	8175	-18.0	-0.1
1834	8196	-17.9	-0.5
1838	8216	-17.9	-0.2
1843	8236	-17.9	-1.0
1847	8257	-18.0	0.4
1852	8277	-17.0	-0.3
1856	8298		
1861	8318	-16.8	0.0
1865	8339	-17.0	0.0
1870	8359	-16.8	0.8
1875	8379	-16.9	0.2
1879	8400	-16.8	0.4
1884	8420	-17.1	0.4
1888	8441	-17.0	0.4
1893	8461	-16.7	0.2
1897	8481	-17.1	0.5
1902	8502	-17.1	0.7
1906	8522	-16.8	0.4
1911	8543	-16.9	0.1
1915	8563	-17.0	0.1
1920	8583	-16.9	0.0
1924	8604	-17.3	0.0
1929	8624	-17.4	-0.2
1933	8645	-17.0	-0.5

1938	8665	-16.8	-0.2
1943	8686	-17.2	-0.1
1947	8706	-17.1	0.2
1952	8727	-16.8	0.7
1956	8748	-16.4	0.5
1961	8769	-16.5	0.2
1966	8789	-16.6	0.3
1970	8810	-16.6	0.4
1975	8831	-16.3	0.8
1979	8851	-16.2	0.7
1984	8872	-16.4	0.7
1989	8893	-16.3	0.5
1993	8914	-16.5	0.3
1998	8934	-16.5	0.5
2002	8952	-16.7	-0.2
2006	8973	-16.5	0.3
2011	8994	-16.6	0.4
2016	9014	-17.1	1.0
2020	9035	-16.7	1.5
2025	9056	-16.8	1.0
2029	9077	-17.5	0.3
2034	9097	-17.5	0.3
2039	9118	-17.3	0.7
2043	9139	-17.1	0.6
2048	9159	-16.9	0.8
2052	9180	-16.7	0.5
2057	9201	-16.8	0.5
2062	9222	-17.0	0.7
2066	9242	-17.6	0.5
2071	9263	-17.3	0.9
2075	9284	-17.0	0.4
2080	9304	-17.1	0.4
2085	9325	-17.1	0.7
2089	9346	-17.9	0.5
2094	9366	-17.8	0.7
2098	9387	-16.9	0.9
2103	9408	-17.4	0.7
2108	9429	-17.3	0.8
2112	9449	-17.2	0.6

2117	9470	-17.0	0.4
2121	9491	-17.5	0.7
2126	9511	-17.6	1.2
2131	9532	-17.6	0.9
2135	9553	-17.7	0.2
2140	9574	-17.6	0.7
2144	9594	-18.2	0.6
2145	9598	-18.0	0.6
2149	9615	-17.8	0.4
2150	9619	-16.8	1.4
2151	9623	-17.0	0.8
2152	9627	-17.3	0.7
2153	9632	-17.2	-0.1
2154	9636	-16.8	0.8
2155	9640	-17.0	0.8
2156	9648	-17.6	0.6
2157	9652	-17.1	0.2
2158	9656	-17.4	0.2
2159	9661	-18.1	-0.3
2160	9665	-17.2	-0.3
2161	9669	-17.1	0.2
2162	9673	-17.0	0.2
2163	9677		
2167	9698	-17.1	-0.1
2172	9719	-17.1	-0.2
2177	9739	-17.1	-0.1
2181	9760	-17.0	-0.1
2186	9781	-17.0	0.3
2190	9801	-17.3	0.0
2194	9818	-16.8	0.1
2199	9838	-17.0	0.0
2203	9858	-17.2	0.5
2208	9879	-17.3	0.3
2212	9899	-17.3	0.0
2217	9920	-17.5	0.3
2221	9940	-16.8	0.7
2225	9957	-16.5	0.7
2226	9960	-16.7	0.4
2230	9981	-15.8	1.1

2235	10001	-17.0	-0.7
2239	10022	-17.3	1.2
2244	10042	-17.1	0.8
2248	10063	-16.6	0.6
2253	10083	-16.8	-0.8
2257	10103	-16.6	-0.5
2262	10124	-15.7	1.0
2267	10144	-15.9	1.1
2271	10165	-15.7	0.9
2276	10185	-15.9	0.8
2277	10189	-15.4	0.5
2277	10193	-16.4	0.2
2278	10197	-16.1	-0.1
2279	10201	-16.6	0.4
2280	10205	-17.1	0.6
2281	10209	-16.7	0.6
2282	10214	-16.7	-0.8
2283	10218	-16.3	-0.8
2284	10222	-15.9	0.8
2285	10226	-16.6	-0.5
2286	10234	-16.5	-0.4
2287	10238	-16.5	-0.7
2288	10242	-16.8	-1.5
2289	10246	-17.0	-0.8
2290	10250	-17.2	-0.6
2291	10254	-16.7	-0.7
2292	10258	-16.4	-0.4
2293	10263	-16.9	-0.3
2294	10267	-17.1	-0.5
2295	10271	-16.7	0.3
2296	10279	-16.3	0.3
2297	10283	-15.6	1.3
2298	10287	-16.1	-0.3
2299	10291	-15.3	1.9
2300	10295	-15.3	1.2
2301	10299	-16.1	0.9
2302	10303	-15.9	0.5
2303	10307	-16.3	0.1
2304	10312	-16.6	0.3

2305	10316	-16.7	-0.3
2306	10324	-17.0	-0.8
2307	10328	-17.3	-0.8
2308	10332	-16.8	-1.0
2309	10336	-16.8	0.4
2310	10340	-16.3	-0.2
2311	10344	-16.4	0.6
2312	10348	-16.2	-0.2
2313	10352	-16.5	0.1
2314	10356	-16.2	1.3
2315	10361	-16.0	1.3
2316	10369	-16.3	0.3
2317	10373	-16.5	0.9
2318	10377	-16.8	-0.1
2319	10381	-16.9	1.2
2320	10385	-16.8	0.9
2321	10389	-16.8	1.1
2322	10393	-16.7	1.4
2323	10397	-16.3	2.0
2324	10401	-17.0	1.6
2325	10409	-17.1	1.4
2326	10414	-16.2	1.8
2327	10418	-16.9	1.9
2328	10422	-16.3	2.3
2329	10426	-16.7	3.2
2330	10430	-15.9	1.1
2331	10434	-16.1	1.1
2332	10438	-15.1	1.3
2333	10442	-15.1	1.2
2334	10446	-15.0	1.5
2335	10450	-15.7	0.9
2336	10458	-15.4	0.8
2337	10462	-15.4	0.7
2338	10466	-15.3	0.9
2339	10470	-15.9	0.8
2340	10474	-15.3	1.0
2341	10479	-15.1	1.1
2342	10483	-15.4	1.1
2343	10487	-15.1	0.9

2344	10491	-15.4	0.5
2345	10499	-15.2	0.5
2346	10503	-14.9	0.5
2347	10507	-15.6	0.2
2348	10511	-16.4	0.2
2353	10531	-16.1	-0.1
2357	10551	-16.6	0.4
2362	10572	-17.1	0.6
2366	10592	-16.7	0.6
2371	10612	-16.7	-0.8
2375	10632	-16.3	-0.8
2380	10653	-15.9	0.8
2384	10673	-16.6	-0.5
2389	10693	-16.6	-0.9
2393	10714	-16.5	-0.4
2398	10734	-16.5	-0.7
2402	10754	-16.8	-1.5
2407	10774	-17.0	-0.8
2411	10795	-17.2	-0.6
2416	10815	-16.7	-0.7
2420	10835	-16.4	-0.4
2425	10855	-16.9	-0.3
2429	10876	-17.1	-0.5
2434	10896	-16.7	0.3
2438	10916	-16.6	-0.1
2439	10920	-16.2	-0.2
2440	10924	-16.4	-0.1
2441	10928	-16.4	-0.2
2442	10932	-16.0	0.5
2443	10936	-16.3	0.3
2443	10940	-15.5	0.4
2444	10944	-15.9	0.6
2445	10949	-15.7	0.7
2446	10953	-15.8	1.1
2447	10957	-15.6	1.3
2448	10961	-15.5	1.1
2449	10965	-15.5	-0.4
2450	10969	-15.5	-0.9
2451	10973	-15.9	-1.1

2452	10977	-16.1	-0.3
2453	10985	-15.2	1.8
2454	10989	-15.0	1.7
2455	10993	-14.6	2.0
2456	10997	-15.3	1.9
2457	11001	-15.0	1.7
2458	11005	-15.0	1.5
2459	11009	-15.2	1.5
2460	11013	-15.4	1.3
2461	11017	-15.3	1.2
2461	11021		
2462	11026	-15.3	1.0
2463	11030	-15.5	0.8
2464	11034	-15.6	0.8
2465	11038	-16.1	0.9
2466	11042	-16.0	0.7
2467	11046	-15.7	0.9
2468	11050	-15.1	1.2
2469	11054	-15.2	1.1
2470	11058	-15.9	0.5
2474	11078	-16.3	0.1
2479	11099	-16.6	0.3
2483	11119	-16.7	-0.3
2488	11140	-16.5	-0.9
2492	11160	-17.0	-0.8
2497	11181	-17.3	-0.8
2501	11201	-16.8	-1.0
2506	11221	-16.8	0.4
2510	11242	-16.3	-0.2
2515	11262	-16.4	0.6
2519	11283	-16.2	-0.2
2524	11303	-16.5	0.1
2528	11323	-16.2	1.3
2533	11344	-16.0	1.3
2538	11364	-16.7	0.1
2542	11385	-16.3	0.3
2547	11405	-16.5	0.9
2551	11425	-16.8	-0.1
2556	11446	-16.9	1.2

2560	11466	-16.8	0.9
2565	11487	-16.8	1.1
2569	11507	-16.7	1.4
2574	11528	-16.3	2.0
2578	11548	-17.0	1.6
2583	11568	-17.6	1.7
2587	11589	-17.1	1.4
2592	11609	-16.2	1.8
2596	11630	-16.9	1.9
2601	11650	-16.3	2.3
2606	11670	-16.7	3.2
2610	11691		
2615	11711	-16.3	-1.5
2619	11732	-15.7	-0.5
2624	11752	-16.2	0.2
2628	11772	-16.0	-1.4
2633	11793		
2637	11813		
2642	11834	-15.5	-3.4
2646	11854	-15.3	-3.8
2651	11874		
2655	11895	-16.0	-3.4
2660	11915	-16.1	-3.2
2664	11936	-16.7	-3.9
2669	11956	-16.4	-3.3
2674	11977	-15.6	-2.0
2678	11997	-15.7	-3.2
2683	12017	-16.6	-3.8
2687	12038		
2692	12058		
2696	12079	-16.9	-3.7
2701	12099		
2705	12119	-16.4	-3.8
2710	12140	-17.7	-4.1
2714	12160	-15.1	-1.7
2719	12181	-15.4	-1.6
2723	12201	-16.1	-2.2
2728	12221	-17.0	-3.3
2732	12242	-16.6	-0.7

2737	12262	-17.1	-1.3
2742	12283	-14.5	-0.5
2746	12303	-13.4	0.6
2751	12323	-15.2	-0.7
2755	12344	-15.6	-2.0
2760	12364	-16.4	-2.4
2764	12385	-16.5	-1.0
2769	12405	-14.8	-1.4
2773	12426	-16.0	-3.2
2778	12446	-14.8	-1.5
2782	12466	-15.1	-1.5
2787	12487	-16.3	-3.2
2791	12507	-16.3	-3.6
2796	12528	-14.9	-0.5
2800	12548	-16.8	-2.4
2805	12568	-16.5	-2.6
2810	12589	-16.0	-2.6
2814	12609	-13.0	-0.7
2819	12630	-17.5	-0.5
2823	12650	-17.6	0.1
2828	12670	-17.4	1.0
3276			
3281			
3285			
3290			
3294			
3299		-10.0	0.1
3303			
3308			
3312			
3317			
3322			
3326			
3331			
3335			
3340			
3344			
3349			
3353			

3358			
3363			
3367		-8.7	0.3
3372			
3376			
3381			
3385			
3390			
3394			
3399			
3404			
3408			
3413			
3417			
3422			
3426			
3431			
3435			
3440			
3445			
3449			
3454			
3458			
3463			
3467			
3472			
3476			
3481			
3486			
3490			
3495		-10.3	0.1
3499			
3504			
3508			
3513			
3517			
3522			
3527			
3531			

3536			
3540			
3545			
3549			
3554			
3558			
3563			
3568			
3572			
3577			
3581			
3586			
3590			
3595		-8.6	0.2
3599			